Small-scale clumps in the galactic halo and dark matter annihilation

Veniamin Berezinsky*
INFN, Laboratori Nazionali del Gran Sasso, I-67010 Assergi (AQ), Italy
and Institute for Nuclear Research of the RAS, Moscow, Russia

Vyacheslav Dokuchaev† and Yury Eroshenko‡
Institute for Nuclear Research of the RAS, Moscow, Russia
(Received 24 April 2003; published 20 November 2003)

Production of small-scale dark matter (DM) clumps is studied in the standard cosmological scenario with an inflation-produced primeval fluctuation spectrum. Special attention is given to the three following problems. (i) The mass spectrum of small-scale clumps with $M \lesssim 10^3 M_\odot$ is calculated with the tidal destruction of the clumps taken into account within a hierarchical model of clump structure. Only 0.1–0.5 % of small clumps survive the stage of tidal destruction in each logarithmic mass interval $\Delta \ln M \sim 1$. (ii) The mass distribution of clumps has a cutoff at $M_{\min}$ due to the diffusion of DM particles out of fluctuation and free streaming at later stages. $M_{\min}$ is a model-dependent quantity. In the case that the neutralino, considered as a pure *B*-ino, is a DM particle, $M_{\min} \sim 10^{-8} M_\odot$. (iii) The evolution of the density profile in a DM clump does not result in a singularity because of the formation of the core under the influence of tidal interaction. The radius of the core is $R_c \sim 0.1R$, where R is the radius of the clump. The applications for annihilation of DM particles in the Galactic halo are studied. The number density of clumps as a function of their mass, radius, and distance to the Galactic center is presented. The enhancement of the annihilation signal due to clumpiness, valid for arbitrary DM particles, is calculated. In spite of a small survival probability, the global annihilation signal in most cases is dominated by clumps. For the observationally preferable value of the index of the primeval fluctuation spectrum $n_p \approx 1$, the enhancement of the annihilation signal is described by a factor of 2 to 5 for different density profiles in a clump.

DOI: 10.1103/PhysRevD.68.103003 PACS number(s): 98.35.Gi, 12.60.Jv, 95.35.+d

I. INTRODUCTION

Both analytic calculations [1,2] and numerical simulations [3–5] predict the existence of dark matter clumps in the Galactic halo. The density profile in these clumps according to analytic calculations [6–9] and numerical simulations [4,10] is $\rho(r) \propto r^{-\beta}$. The average density of the dark matter (DM) in Galactic halo itself also exhibits a similar density profile (relative to the Galactic center) in both approaches. The DM profile in clusters of galaxies is discussed in [11] and in references therein. In the analytic approach of Gurevich and Zybin (see the review [9] and references therein) the density profiles are predicted to be universal, with $\beta \approx 1.7-1.9$ for clumps, galaxies, and two-point correlation functions of galaxies. In numerical simulations the density profiles can be evaluated only for relatively large scales due to the limited mass resolution. The value of β differs in different simulations from $\beta = 1.0$ [10] to $\beta = 1.5$ [3] and may be nonuniversal for objects of different mass scales [12]. An attempt at an analytical explanation of the results of the numerical simulations has been performed in [13,14]. The phase-space density profiles of DM halos are investigated in [15].

A central cusp in the Galactic halo and the smaller-scale clumps results in the enhancement of the DM annihilation rate and thus in stronger signals in the form of gamma rays, radio emission, positrons, and antiprotons. The gamma ray and radio signal from the central cusp in the Galactic halo was first discussed in [16,17]. Recently this problem was examined in [18–22]. The enhancement of the DM annihilation rate due to the clumpiness of the DM halo was first pointed out in [1]. Neutralino annihilation in clumps can result in a very large diffuse gamma ray flux [23] in the model of the clumpy DM by Gurevich *et al.* [2]. Calculations of positron and antiproton production in the clumpy DM halo have been performed, e.g., in [18] (see also [24–26]). Recently, the annihilation of DM in the clumps has been studied in [27–32]. The synchrotron flux from DM annihilation products in clumps in the presence of the Galactic magnetic field is considered in [33]. Constraints on the DM clumpiness in the halos from heating of the disk galaxies is examined in [34,35].

The main purpose of this work is evaluation of the enhancement of the annihilation signal due to the presence of the small clumps of DM in the Galactic-halo.

Small-scale self-gravitating dark matter clumps, which will be referred to as DMCs or simply as clumps, may have formed in the early universe due to several mechanisms. These DMCs may be formed (i) by the growth of adiabatic or isothermal fluctuations (originating at inflation) during the matter-dominated epoch; or (ii) from the density fluctuations in models with topological defects (cosmic strings and domain walls) [1]; or (iii) during the radiation-dominated era from nonlinear isothermal fluctuations (originating in phase transitions in the early universe) [36] or from large-amplitude adiabatic fluctuations [37].

*Electronic address: berezinsky@lngs.infn.it
†Electronic address: dokuchaev@inr.npd.ac.ru
‡Electronic address: erosh@inr.npd.ac.ru

In this paper we shall consider only the most conservative case of adiabatic fluctuations which enter the nonlinear stage of evolution in the matter-dominated epoch with an inflation-induced initial power-law power spectrum.

Small-scale clumps are formed only if the fluctuation amplitudes in the spectrum are large enough at the corresponding small scales. The inflation models predict the power-law primeval fluctuation spectrum. If the power-law index $n_p \geqslant 1$, DMCs are formed in a wide range of scales. During the universe expansion the small clumps are captured by the larger ones, and the larger clumps consist of the smaller ones and of continuously distributed DM. A convenient analytic formalism, which describes this hierarchical clustering statistically, is the Press-Schechter theory [38] and its extensions, in particular the ''excursion set'' formalism developed by Bond *et al.* [39] (for a clear introduction, see [40]). However, this theory does not include the important process of tidal destruction of small clumps inside the bigger ones. We take this process into account in Sec. V and obtain the mass function for the small-scale DMCs in the Galactic halo. In the case of a power-law spectrum only a small fraction of the captured clumps survives, but even this small fraction is enough to dominate the total annihilation rate in the Galactic halo.

In the hierarchical theory of large-scale structure formation in the universe the first objects formed have some minimal mass $M_{\min}$. The value of this mass is determined by the spectrum of initial fluctuations and by the properties of DM particles [2,41]. This value is crucial for calculation of the DM annihilation rate. The estimates of $M_{\min}$ existing in the literature for neutralino DM are substantially different, from $M_{\min} \sim 10^{-12} M_\odot$ in [42] to $M_{\min} \sim (10^{-7}-10^{-6}) M_\odot$ in [43]. In Sec. III we present our calculations and discuss the previous results.

The DM annihilation rate crucially depends on the density profile $\rho(r) \propto r^{-\beta}$ of DM particles in a clump and on the distance R_c where the density growth is cut off. This region is called the core. The radius of the core has been estimated in the literature in the different approximations. The estimation $R_c/R \sim \delta_{\rm eq}^3$, where $\delta_{\rm eq}$ is the density fluctuation amplitude at the end of the radiation-dominated epoch, was obtained in [9]. It was found from the behavior of the damped mode of nonlinear fluctuations. A black hole or baryonic core in the center of the DMC can strongly affect the density saturation at $r \to 0$ for a very massive DMC [9,19–21]. Calculations [16,23] of the inward flux of DM particles into the dense central region of a DMC also result, due to annihilation of DM particles, in a very small radius of the central core R_c. The above mentioned process is essential for the formation of the DMC core only in the case of almost perfectly spherically symmetrical clumps.

We shall estimate the radius of the core imposed by tidal interaction, which gives the largest R_c among those known in the literature. In the spherically symmetric self-gravitating clump at the stage of its formation the nondissipative DM particles are moving nearly radially in the oscillation regime. The presence of a nonspherical (tidal) external gravitational field causes the deflection of particle trajectories in the clump from the radial ones. This process prevents the development of the central singularity in a clump and results in the core formation.

During the radiation-dominated epoch the small fluctuations $\delta = \delta\rho/\rho \ll 1$ grow very slowly. In the matter-dominated stage these fluctuations start to grow fast [44] in the regime $\delta \propto t^{2/3}$. Fluctuations get detached from the general cosmological expansion and start contracting after reaching the nonlinear value $\delta \geqslant 1$. These nonlinear fluctuations finally form the DM clumps. Analytic studies of the nonlinear evolution of fluctuations have been performed by many authors. One of the most detailed analytical approaches was developed by Gurevich and Zybin [9]. In this formalism at a certain moment of gravitational contraction the density singularity forms in the center of a nonlinear fluctuation. From this singularity point the density caustics (i.e., the boundary of regions with a different number of streams) expand outward. The secondary caustics appear inside the primary ones and their number increases fast with time. This multistream instability was discovered and studied in detail in [9]. It was demonstrated that the stationary universal density profile $\rho(r) \propto r^{-\beta}$ with $\beta = 1.7-1.9$ is formed as a result of streams mixing. The maximum density of DM particles in a clump is reached at the center.

In our consideration of the clump formation we shall follow for convenience the theoretical scenario of Gurevich and Zybin [9]. However, the effects of tidal interaction, which is the main result of our work, are valid for a much broader class of scenarios.

The processes described above are valid for all DM particles which can be considered as nondissipative. The signal production depends on the annihilation cross section and thus on the nature of the DM particles. However, our strategy is to calculate the enhancement of the signal due to the halo clumpiness in comparison with an isotropic unclumped distribution of DM. As a guide we shall take the neutralino as the DM particle, but essentially our results for enhancement of the annihilation signal are relevant for a wide class of other DM particles.

We perform our calculations for a cosmological model with the matter density $\Omega_m = 0.3$ and the cosmological term $\Omega_\Lambda = 1 - \Omega_m \simeq 0.7$. The presence of the Λ term influences only the value of $\rho_{\rm eq}$ and does not affect the formation of low-mass DMCs. This is because the Λ term contributes negligibly to the total cosmological density at time scales when the low-mass DMCs formation occurs. We shall use the index ''eq'' for the values at the moment of equality (i.e., the transition from the radiation-dominated to the matter-dominated epoch). We shall use the Hubble constant 70 $\mathrm{km\,s^{-1}\,Mpc^{-1}}$.

II. ENHANCEMENT OF ANNIHILATION SIGNAL DUE TO CLUMPS

Let us consider a DM clump with the internal density profile $\rho_{\rm int}(r)$ and a total mass $M = \int 4\pi r^2 \rho_{\rm int}(r) dr$. The annihilation rate in a single clump is given by

$$\dot{N}_{\rm cl} = 4\pi \int_0^\infty r^2 dr\, \rho_{\rm int}^2(r) m_\chi^{-2} \langle \sigma_{\rm ann} v \rangle = \frac{3}{4\pi} \frac{\langle \sigma_{\rm ann} v \rangle}{m_\chi^2} \frac{M^2}{R^3} S, \tag{1}$$

where m_χ is the mass of a DM particle (not necessarily the neutralino), v is the relative velocity of two DM particles at the collision, $\sigma_{\rm ann}$ is the annihilation cross section and R is the virial radius of a clump. The function S is determined by Eq. (1) and depends on the DM distribution in a clump, in particular, $S=1$ for the simplest case of a uniform clump, when $\rho_{\rm int}(r)=$const at $r\leqslant R$ and $\rho_{\rm int}(r)=0$ at $r>R$.

The expansion of $\langle\sigma_{\rm ann}v\rangle$ over the relative velocity v of two DM particles has the form

$$\langle\sigma_{\rm ann}v\rangle=a+bv^2+cv^4+\cdots, \tag{2}$$

where a has a contribution from the s-wave amplitude only, and b from both s and p waves. Since v is very small, $\langle\sigma_{\rm ann}v\rangle$ can be put outside the integral in Eq. (1).

We shall use the following parametrization of the density profile in a clump:

$$\rho_{\rm int}(r)=\begin{cases}\rho_c, & r<R_c,\\ \rho_c\left(\dfrac{r}{R_c}\right)^{-\beta}, & R_c<r<R,\\ 0, & r>R.\end{cases} \tag{3}$$

Using $\rho_{\rm int}(r)$ from Eq. (3) it is easy to calculate S from Eq. (1) as

$$S(x_c,\beta)=\frac{(3-\beta)^2}{3(2\beta-3)}\left(\frac{2\beta}{3}x_c^{3-2\beta}-1\right)\left(1-\frac{\beta}{3}x_c^{3-\beta}\right)^{-2}, \tag{4}$$

where $x_c=R_c/R$. Another approach to the parametrization of the clump structure was used in [29].

The clumps in the Galactic halo are distributed over at least three parameters, mass M, radius R, and distance from the Galactic center, l: $n_{\rm cl}(M,R,l)$. This distribution can also depend on the parameters that describe the internal structure of the clumps, β and x_c, from Eq. (3). We shall discuss this dependence in Sec. IV. In particular, it will be demonstrated that $x_c=x_c(M,R)$, while β is a universal constant. Thus the differential number density of DMCs in the halo can be written as

$$dN_{\rm cl}=n_{\rm cl}(l,M,R)d^3l\,dM\,dR. \tag{5}$$

The observed signal at the position of the Earth from DM particle annihilation in the clumps is proportional to the quantity

$$I_{\rm cl}=\frac{1}{4\pi}\int_0^\pi d\zeta\sin\zeta\int_0^{r_{\rm max}(\zeta)}\frac{2\pi r^2dr}{r^2}\int_{M_{\rm min}}^{M_{\rm max}}dM\int_{R_{\rm min}}^{R_{\rm max}}dR \times n_{\rm cl}(l(\zeta,r),M,R)\dot{N}_{\rm cl}(M,R), \tag{6}$$

where r is the distance from the Sun (Earth) to a clump and ζ is the angle between the line of observation and the direction to the Galactic center. The distance l between a clump and the Galactic center can be given in terms of r, $r_\odot$ (distance from the Sun to the Galactic center), and ζ as $l(\zeta,r)=(r^2+r_\odot^2-2rr_\odot\cos\zeta)^{1/2}$, and the maximum distance from the Sun to the outer halo border in the direction of ζ, $r_{\rm max}(\zeta)=(R_H^2-r_\odot^2\sin^2\zeta)^{1/2}$, where $R_H\sim100$ kpc is the Galactic halo virial radius and $r_\odot=8.5$ kpc is the distance from the Sun to the Galactic center.

An additional annihilation signal is given by unclumpy DM in the halo with homogeneous (i.e., smoothly spread) density $\rho_{\rm DM}(l)$, where l is the distance to the Galactic center:

$$I_{\rm hom}=\frac{\langle\sigma_{\rm ann}v\rangle}{2}\int_0^\pi d\zeta\sin\zeta\int_0^{r_{\rm max}(\zeta)}dr\,\rho_{\rm DM}^2[l(\zeta,r)]/m_\chi^2. \tag{7}$$

The *enhancement* η of the signal due to the presence of clumps is given by

$$\eta=\frac{I_{\rm cl}+I_{\rm hom}}{I_{\rm hom}}. \tag{8}$$

This quantity describes the global enhancement of the annihilation signal observed at the Earth (e.g., the flux of radio, gamma, and neutrino radiations) as compared with the usual calculations from annihilation of unclumpy DM. From Eqs. (8), (7), and (6) one can see that the enhancement η does not depend on the properties of DM particles, in particular, on the annihilation cross section and is fully determined by the parameters of DM clumpiness. Further exact calculations in this paper will be performed using Eqs. (6)–(8), but now we shall turn to the approximate expression for η.

We shall accept now the simplifying assumptions. We assume that the space density of clumps in the halo, $n_{\rm cl}(l)$, is proportional to the unclumpy DM density $\rho_{\rm DM}(l)$: $n_{\rm cl}(l)=\xi\rho_{\rm DM}(l)/M$ with $\xi\ll1$. This assumption holds with good accuracy for the small-scale clumps. In contrast, the distribution of large-scale clumps obtained in the numerical simulations [45] is rather different from the density distribution of the small clumps, especially in a central part of the halo because of the tidal disruption of clumps there. However, the clump signal is determined mostly by clumps of the minimal mass. We neglect here the distribution of clumps over M and R. Instead we shall use a mean density of DM particles inside a clump $\overline{\rho}_{\rm int}=3M/4\pi R^3$. Finally, we shall introduce for convenience the effective density of DM particles in the halo defined as

$$\tilde{\rho}_{\rm DM}\equiv\frac{\int_0^\pi d\zeta\sin\zeta\int_0^{r_{\rm max}(\zeta)}dr\,\rho_{\rm DM}^2[l(\zeta,r)]}{\int_0^\pi d\zeta\sin\zeta\int_0^{r_{\rm max}(\zeta)}dr\,\rho_{\rm DM}[l(\zeta,r)]}. \tag{9}$$

As a result, we obtain for an enhancement factor the convenient *estimate*

$$\eta\approx1+\xi S(x_c,\beta)\frac{\overline{\rho}_{\rm int}}{\tilde{\rho}_{\rm DM}}, \tag{10}$$

where ξ is the fraction of DM in the form of clumps (see above) and $S(x_c,\beta)$ is given by Eq. (4). For typical parameters (see details in the following sections), $n_p\simeq1$, $\beta\simeq1.8$, $x_c\simeq0.05$, $S(x_c,\beta)\simeq5$, $\tilde{\rho}_H\sim\rho_{\rm DM}(r_\odot)\sim0.3$ GeV cm^{-3}, $\overline{\rho}_{\rm int}\sim2\times10^{-22}$ g cm^{-3}, $\xi\sim0.001$, the numerical estimate $\eta\sim3$ follows from Eq. (10).

III. CLUMPS OF MINIMAL MASSES

The number of clumps in the halo increases at small clump masses M, and the signal from clumps $I_{\rm cl}$ crucially depends on $M_{\rm min}$ in the clump distribution, as Eq. (6) shows. The value of $M_{\rm min}$ is determined by a leakage of DM particles from the overdense fluctuations in the early universe. We shall first describe this process qualitatively and then present numerical calculations.

Cold dark matter (CDM) particles at high temperature $T > T_f \sim 0.05 m_\chi$ are in thermodynamical (chemical) equilibrium with cosmic plasma, when their number density is determined by temperature. After freezing at $t > t_f$ and $T < T_f$, the DM particles remain for some time in *kinetic* equilibrium with the plasma, when the temperature of the CDM particles T_χ is equal to the temperature of the plasma T, but the number density n_χ is determined by the freezing concentration and expansion of the universe. At this stage the CDM particles are not perfectly coupled to the cosmic plasma. Collisions between a CDM particle and fast particles of the ambient plasma result in exchange of momenta and a CDM particle diffuses in space. Due to diffusion the DM particles leak from the small-scale fluctuations and thus their distribution has a cutoff at the minimal mass M_D.

When the energy relaxation time for DM particles $\tau_{\rm rel}$ becomes larger than the Hubble time $H^{-1}(t)$, the DM particles get out of kinetic equilibrium. This condition determines the time of kinetic decoupling t_d. At $t \geqslant t_d$ the CDM particles are moving in the free streaming regime and all fluctuations on the scale of

$$\lambda_{\rm fs} = a(t_0) \int_{t_d}^{t_0} \frac{v(t')dt'}{a(t')} \tag{11}$$

and smaller are washed away [here $a(t)$ is the scaling factor of the expanding universe and $v(t)$ is the velocity of a DM particle at epoch t]. The corresponding minimal mass at epoch t_0,

$$M_{\rm fs} = \frac{4\pi}{3} \rho_\chi(t_0) \lambda_{\rm fs}^3, \tag{12}$$

is much larger than M_D. Numerical calculations below (for the neutralino) show that M_D is close to $M_{\rm min}$ from [42] and $M_{\rm fs}$ to $M_{\rm min}$ from [43].

The calculation of the minimal mass $M_{\rm min}$ in the mass spectrum of fluctuations is obviously model dependent. As the DM particle we shall consider the neutralino χ, for which we take the pure B-ino state ($\chi = \tilde{B}$). As the calculations below show, the temperature of kinetic decoupling for a reasonable range of parameters is $T_d \sim 100$ MeV, and thus we can consider a cosmic plasma consisting of relativistic electrons, positrons, neutrinos, and photons in thermal equilibrium.

The cross sections for scattering of B-inos off the left (right) electron and left neutrino are given in Appendix A. The cross section for $\nu\chi$ scattering is given by Eq. (A5) and for $e\chi$ scattering it is 17 times larger, if we assume equal masses of selectrons and sneutrinos (we shall use $\tilde{m}$ for both the left and right selectron and sneutrino masses, and $\tilde{M}^2 = \tilde{m}^2 - m_\chi^2$).

First of all we shall calculate the moment t_d and temperature T_d of kinetic decoupling of the neutralino, using the condition

$$\frac{1}{\tau_{\rm rel}} \simeq H(t), \tag{13}$$

where $H(t) = 1/(2t)$ is the Hubble constant and $\tau_{\rm rel}(T)$ is the energy relaxation time for the neutralino at the temperature of the electron-neutrino gas T. The relaxation time $\tau_{\rm rel}$ is determined by collisions of neutralinos with fermions ν_L, e_L, and e_R. The neutralino can be considered as a particle at rest because the rest system coincides with the center-of-mass system with an accuracy of order $\sqrt{T/m_\chi}$. Let δp be the neutralino momentum obtained in one scattering:

$$(\delta p)^2 = 2\omega^2(1 - \cos\theta), \tag{14}$$

where ω and θ are the neutrino energy and scattering angle, respectively.

Let us introduce the number density of relativistic fermions with one polarization and with energy ω:

$$n_0(\omega) = \frac{1}{2\pi^2} \frac{\omega^2}{e^{\omega/T} + 1}. \tag{15}$$

Then for the energy relaxation time $\tau_{\rm rel}$ we have

$$\frac{1}{\tau_{\rm rel}} = \frac{1}{E_k} \frac{dE_k}{dt} = \frac{40}{2E_k m_\chi} \int d\Omega \int d\omega\, n_0(\omega) \left(\frac{d\sigma_{\rm el}}{d\Omega} \right)_{f_L \chi} (\delta p)^2, \tag{16}$$

where $E_k \simeq (3/2)T$ is the mean kinetic energy of the neutralinos, and $(d\sigma_{\rm el}/d\Omega)_{f_L\chi}$ is given by Eq. (A5). The number 40 in Eq. (16) is obtained by counting degrees of freedom: three neutrinos and antineutrinos (or ν_L^c in the case of Majorana neutrinos) give six, e_L and e_L^c give two, and two right (singlet) states for electrons and positrons gives 34, because their cross sections are 17 times larger.

After integration in Eq. (16) we obtain

$$\frac{1}{\tau_{\rm rel}} = \frac{40\Gamma(7)\alpha_{\rm e.m.}^2}{9\pi \cos^4\theta_W} \frac{T^6}{\tilde{M}^4 m_\chi}. \tag{17}$$

Using Eq. (13) and the connection between the age and temperature of the universe,

$$t = \frac{2.42}{\sqrt{g_*}} \left(\frac{T}{1\ \text{MeV}} \right)^{-2}\ \text{s}, \tag{18}$$

where g_* is the number of degrees of freedom, we obtain numerically

$$t_d = 3.5\times 10^{-5}\left(\frac{m_\chi}{100\ \mathrm{GeV}}\right)^{-1/2}\left(\frac{\tilde{M}}{1\ \mathrm{TeV}}\right)^{-2}\left(\frac{g_*}{10}\right)^{-3/4}\ \mathrm{s}, \tag{19}$$

and

$$T_d = 150\left(\frac{m_\chi}{100\ \mathrm{GeV}}\right)^{1/4}\left(\frac{\tilde{M}}{1\ \mathrm{TeV}}\right)\left(\frac{g_*}{10}\right)^{1/8}\ \mathrm{MeV}. \tag{20}$$

We shall present in this section calculations made in a physically transparent way, considering the diffusive leaking of neutralinos at the stage of kinetic equilibrium and free streaming when neutralinos get out of kinetic equilibrium. In Appendix B we shall study both stages together in the formalism of the kinetic equation, as was done in [42]. Although our methods are not identical, their comparison implies that the absence of free streaming is responsible for the contradiction with different $M_{\min}$ discussed above. The independent approach in Appendix B confirms the results obtained below.

A. Diffusion cutoff of the mass spectrum

We can come now to the calculation of M_D, the minimal mass in the fluctuation spectrum caused by diffusion of neutralinos out of an overdense fluctuation. We calculate the diffusion coefficient using the method given in [46] (Sec. 12). Consider a neutralino moving with a nonrelativistic velocity $\vec{v}$. In the rest system of this particle the momentum distribution of relativistic fermions is anisotropic:

$$n(\vec{p})d^3p = \frac{d\Omega_\alpha p^2 dp}{(2\pi)^3}\,\frac{1}{e^{p(1+v\,\cos\alpha)/T}+1}, \tag{21}$$

where α is the angle between the directions of $\vec{v}$ and the momentum of the incoming fermion.

The momentum transfer in a single scattering equals $\vec{p}(1-\cos\theta)$ after averaging over the azimuthal angles.

The corresponding friction force experienced by the neutralino is

$$\vec{f}_r = 40\int d\Omega_\theta \int d^3p\, n(\vec{p})\left(\frac{d\sigma_{\mathrm{el}}}{d\Omega_\theta}\right)_{f\chi}\vec{p}(1-\cos\theta) = -B^{-1}\vec{v}, \tag{22}$$

where B is the particle mobility and the factor 40 takes into account scattering on all fermions as in Eq. (17). Then the diffusion coefficient is

$$D = BT = \frac{3\pi\cos^4\theta_W \tilde{M}^4}{40\Gamma(6)\alpha_{\mathrm{e.m.}}^2 T^5}. \tag{23}$$

Diffusion equation in the comoving system has the form

$$\frac{\partial\delta(\vec{x},t)}{\partial t} = \frac{D(t)}{a^2(t)}\Delta_{\vec{x}}\delta(\vec{x},t). \tag{24}$$

The diffusion coefficient $D(t)$ is time dependent because of $T(t)$. The solution of Eq. (24) for the Fourier component is

$$\delta_{\vec{k}}(t) = \delta_{\vec{k}}(t_f)\exp\{-k^2 C g_*^{5/4}\tilde{M}^4(t^{5/2}-t_f^{5/2})\}, \tag{25}$$

where $C=$const. The factor $Cg_*^{5/4}\tilde{M}^4(t^{5/2}-t_f^{5/2})$ in front of k^2 in Eq. (25) is the diffusion length squared $\lambda_D^2(t)/a^2(t)$ in the comoving coordinates. This value determines the minimal mass in the density perturbation spectrum due to diffusion of neutralinos from a fluctuation:

$$M_D = \frac{4\pi}{3}\rho_\chi(t_d)\lambda_D^3(t_d) = 4.3\times 10^{-13}\left(\frac{m_\chi}{100\ \mathrm{GeV}}\right)^{-15/8}\times\left(\frac{\tilde{M}}{1\ \mathrm{TeV}}\right)^{-3/2}\left(\frac{g_*}{10}\right)^{-15/16} M_\odot. \tag{26}$$

The functional dependence of Eq. (25) and numerical value of Eq. (26) obtained in the diffusion approximation coincide with the corresponding results obtained by a different method in [42].

B. Free streaming cutoff of the mass spectrum

We shall consider now the free streaming cutoff of the mass spectrum qualitatively described in the beginning of this section. We gave there an estimate of the minimal mass due to free streaming. In the accurate calculations below we shall take into account the angular and velocity distribution of leaking neutralinos, and the exact dependence of $a(t)$ at age $\sim t_{\mathrm{eq}}$, which affect the value of M_{fs}.

After the moment of kinetic decoupling t_d, neutralinos move freely in the expanding universe background, $a(t)d\vec{x} = \vec{v}(t)dt$, where $\vec{x}$ is the comoving particle coordinate. The coordinates $\vec{x}$ at some moment t are determined by the initial coordinates $\vec{q}$ and velocity $\vec{v}_d$ at the moment of kinetic decoupling t_d:

$$\vec{x} = \vec{f}(\vec{q},\vec{v}_d,t) = \vec{q} + \int_{t_d}^{t}\frac{\vec{v}(t')dt'}{a(t')} = \vec{q} + g(t)\vec{v}_d, \tag{27}$$

where

$$g(t) = a(t_d)\int_{t_d}^{t}\frac{dt'}{a^2(t')}, \tag{28}$$

$\vec{v}(t) = \vec{v}_d a(t_d)/a(t)$ for nonrelativistic particles. Now for the neutralino number density at the point $\vec{x}$ we have

$$n(\vec{x},t) = \int d^3v_d\,\phi(\vec{v}_d)\sum_{\vec{q}_*} n(\vec{q}_*,t_d)\left|\frac{D\vec{f}}{D\vec{q}}\right|_{\vec{q}=\vec{q}_*} = \int d^3v_d\,\phi(\vec{v}_d)\int d^3q\, n(\vec{q},t_d)\,\delta^{(3)}(\vec{x}-\vec{f}(\vec{q},\vec{v}_d,t)), \tag{29}$$

where $\delta^{(3)}$ is the Dirac delta function, $D\vec{f}/D\vec{q}$ is the Jacobian, and $\phi(\vec{v}_d)$ is the neutralino velocity distribution func-

tion at the moment t_d. The summation in Eq. (29) goes over all roots $\vec{q}_*$ of the equation $\vec{x}=\vec{f}(\vec{q},\vec{v}_d,t)$ from Eq. (27). This sum in fact has only one term because the function $f(\vec{q},\vec{v}_d,t)$ in Eq. (27) is a single-valued one.

From Eqs. (27) and (29) we find the Fourier component

$$n_{\vec{k}}(t)=n_{\vec{k}}(t_d)\int d^3v_d\phi(\vec{v}_d)e^{-i\vec{k}\vec{v}_d g(t)}. \tag{30}$$

Assuming the velocity distribution at the moment of decoupling $\phi(\vec{v}_d)$ to be Maxwellian

$$\phi(\vec{v}_d)=\left(\frac{m_\chi}{2\pi T_d}\right)^{3/2}\exp\left\{-\frac{m_\chi v_d^2}{2T_d}\right\}, \tag{31}$$

we obtain

$$n_{\vec{k}}(t)=n_{\vec{k}}(t_d)e^{-(1/2)k^2g^2(t)T_d/m_\chi}, \tag{32}$$

i.e., up to the moment t all perturbations are washed out by free streaming inside the physical length scale

$$\lambda_{\rm fs}(t)=a(t)g(t)\left(\frac{T_d}{m_\chi}\right)^{1/2}. \tag{33}$$

This length scale corresponds to the clump of minimal mass

$$M_{\rm fs}(t)=\frac{4\pi}{3}\rho_\chi(t)\lambda_{\rm fs}^3(t), \tag{34}$$

where $\rho_\chi(t)=\rho_{\rm eq}a_{\rm eq}^3/a^3(t)$. The time dependence of $M_{\rm fs}(t)$ is regulated by $a(t)$. In the radiation-dominated epoch, $M_{\rm fs}(t)$ grows logarithmically with time. This growth is saturated in the matter-dominated epoch. The resulting $M_{\rm min}$ at t_0 can easily be calculated using $a(t)$ as the solution of the Friedmann equation:

$$a(\eta)=a_{\rm eq}\left[2\frac{\eta}{\eta_*}+\left(\frac{\eta}{\eta_*}\right)^2\right],$$

$$t=a_{\rm eq}\eta_*\left[\left(\frac{\eta}{\eta_*}\right)^2+\frac{1}{3}\left(\frac{\eta}{\eta_*}\right)^3\right]. \tag{35}$$

In these equations $\eta_*^{-2}=2\pi G\rho_{\rm eq}a_{\rm eq}^2/3$, $a_{\rm eq}$ is the value of the scaling factor at the moment $t_{\rm eq}$,

$$\rho_{\rm eq}=\rho_0(1+z_{\rm eq})^3=1.1\times10^{-19}\left(\frac{h}{0.7}\right)^8\left(\frac{\Omega_m}{0.3}\right)^4\ {\rm g\,cm^{-3}}, \tag{36}$$

$1+z_{\rm eq}=2.35\times10^4\Omega_m h^2$, and $\rho_0=1.9\times10^{-29}\Omega_m h^2$ g cm^{-3}. The presence of the cosmological constant Λ affects only the value $\rho_{\rm eq}$ and does not influence the evolution $M_{\rm fs}(t)$ because the contribution of Λ to the total cosmological density is negligible at small t. Putting Eq. (35) into Eq. (28), we find after integration

$$M_{\rm min}=\frac{\pi^{1/4}}{2^{19/4}3^{1/4}}\frac{\rho_{\rm eq}^{1/4}t_d^{3/2}}{G^{3/4}}\left(\frac{T_d}{m_\chi}\right)^{3/2}\ln^3\left\{\frac{24}{\pi G\rho_{\rm eq}t_d^2}\right\}. \tag{37}$$

Using Eqs. (19) and (20) we obtain numerically

$$M_{\rm min}=1.5\times10^{-8}\left(\frac{m_\chi}{100\ {\rm GeV}}\right)^{-15/8}\left(\frac{\tilde{M}}{1\ {\rm TeV}}\right)^{-3/2}\times\left(\frac{g_*}{10}\right)^{-15/16}\left(\frac{\Lambda^*}{83}\right)^3 M_\odot, \tag{38}$$

where Λ^* is the logarithm from Eq. (37).

Our calculations agree well with [43] as far as the most important quantity T_d is concerned (the scattering cross section is involved only there). The calculation of $M_{\rm min}$ from T_d in our case involves nonradial propagation of neutralinos in a fluctuation and their distribution over velocities, Eqs. (27)–(32). We include also the accurate time dependence of the scaling factor $a(t)$. The calculations in [43] follow the semiquantitative scheme described at the beginning of Sec. III. At this stage of the calculations we have a difference described by a factor of 7.

In conclusion, in this section we have considered two processes of washing out the cosmological density perturbations in a neutralino gas. The first process is the neutralino diffusion due to scattering off neutrinos, electrons, and positrons. This process is effective until neutralinos are in kinetic equilibrium with the cosmological plasma. Up to the moment of decoupling t_d all perturbations with mass $M<M_D\simeq(10^{-13}-10^{-12})M_\odot$ are washed out. The second process is neutralino free streaming. Starting later, at $t>t_d$, it washes out the larger perturbations with $M\leqslant M_{\rm fs}$ and determines $M_{\rm min}$ in the clump mass distribution at the present epoch, as given by Eq. (38).

IV. CORE OF A DARK MATTER CLUMP

In this section we shall consider smearing of the singular density profile in a clump due to tidal forces and calculate the radius R_c of the core produced.

Clumps, as well as galaxies, originate near the maxima in cosmological density perturbations $\delta(\vec{r})=[\rho(\vec{r})-\overline{\rho}]/\overline{\rho}$. At the matter-dominated stage the density perturbations grow as $\delta\propto t^{2/3}$. In the nonlinear regime $\delta\gtrsim1$, a multiflux instability develops in a clump, and a singular density profile is formed [9]. If the velocity field in the central part of the clump is disturbed and becomes weakly nonradial, the flow is overturned, a singularity does not form, and the density profile is smoothed. In [9] the core radius is estimated as $x_c\simeq\delta_{\rm eq}^3\ll1$ by consideration of the perturbation of the velocity field due to the damped mode of the cosmological density perturbations. Here $\delta_{\rm eq}$ is the initial density fluctuation value at the end of the radiation-dominated epoch. In [23] the core is produced for a spherically symmetric clump by inverse flow caused by annihilation of DM particles. We shall show here that these phenomena are not the main effects and that a much stronger disturbance of the velocity field in the core is produced by tidal forces. These forces originate due to the nonsphericity of the perturbation considered and the presence of other fluctuations nearby, including a fluctuation on a larger scale in which the considered fluctuation can be submerged.

Core formation in a fluctuation begins at the linear stage of evolution and continues at the beginning of the nonlinear stage. The tidal forces diminish with time t [see Eq. (53) below], and the duration of this phase is proportional to t. Once the core is produced it is not destroyed in the following evolution. The stage of core formation continues approximately from $t_{\rm eq}$ to the time of maximal expansion t_s and a little above, when a clump is detached from the expansion of the universe and evolves in the nonlinear regime. Soon after this period, a clump enters the hierarchical stage of evolution, when the tidal forces can destroy it, but surviving clumps retain their cores.

Let us expand the gravitational potential in a series near the maximum of the density fluctuation taken as $\vec{r}=\vec{0}$ at arbitrary time t during the *linear* growth of density perturbations:

$$\phi(\vec{r},t)=\phi_0+\left.\frac{\partial\phi}{\partial r^i}\right|_0 r^i+\frac{1}{6}\Phi_{ll}|_0\delta_{ij}r^ir^j+\frac{1}{2}T_{ij}|_0r^ir^j+\cdots, \tag{39}$$

where

$$\Phi_{ij}=\frac{\partial^2\phi(\vec{r})}{\partial r^i\partial r^j}, \quad T_{ij}=\Phi_{ij}-\frac{1}{3}\Phi_{ll}\delta_{ij}. \tag{40}$$

The first term of the series in Eq. (39) does not influence the particle motion. The second term is zero as a condition of maximum density. The third term describes the spherically symmetric part of the potential (including the potential of the homogeneous background) and also the perturbation potential. It governs the radial motion of the particles. According to the Poisson equation one has

$$\Phi_{ll}=\Delta\phi(\vec{r})=4\pi G\overline{\rho}[1+\delta(\vec{r})]. \tag{41}$$

Finally, the fourth term, which contains the traceless matrix T_{ij}, describes the tidal forces. They disturb the radial motion of the particles and result in production of the core.

We shall start with definitions and notation. We assume that density perturbations $\delta(\vec{r})$ are Gaussian with a power spectrum $P(k)$:

$$\langle\delta^*_{\vec{k}}\delta_{\vec{k}'}\rangle=(2\pi)^3P(k)\delta_D^{(3)}(\vec{k}-\vec{k}'), \quad \delta_{\vec{k}}=\int\delta(\vec{r})e^{i\vec{k}\vec{r}}d^3r, \tag{42}$$

where $\delta_D^{(3)}(\vec{k}-\vec{k}')$ is the Dirac delta function and angular brackets correspond to ensemble averaging. The power spectrum $P_{\rm eq}(k)$ at time $t_{\rm eq}$ is connected with the primordial power spectrum $P_p(k)$ (at the epochs before horizon crossing) by the relation $P_{\rm eq}(k)=P_p(k)T^2(k)$, where $T(k)$ is the transfer function for cold dark matter (see, e.g., [47]).

From Eq. (41) it follows that the power spectrum $P_\Phi(k)$ of potential perturbations is related to $P(k)$ as

$$P_\Phi(k)=(4\pi)^2G^2\overline{\rho}^2k^{-4}P(k). \tag{43}$$

Let us introduce the moments of the spectrum $P(k)$:

$$\sigma^2_{(j)}=\frac{1}{2\pi^2}\int_0^\infty k^2dk\,P(k)k^{2j}, \tag{44}$$

and the similar moments $s^2_{(j)}$ for the perturbation field of the gravitational potential. Calculating the divergent moments for a given mass M we assume the smoothing procedure of [47].

From Eq. (43) it follows that

$$s^2_{(j)}=(4\pi)^2G^2\overline{\rho}^2\sigma^2_{(j-2)} \tag{45}$$

for $j\geqslant 2$. Let us define $\zeta_{ij}=\partial^2\delta(\vec{r})/\partial r^i\partial r^j$. Then according to [47] its mean value over the ensemble is

$$\langle\zeta_{ij}\zeta_{kl}\rangle=\frac{\sigma^2_{(2)}}{15}(\delta_{ij}\delta_{kl}+\delta_{ik}\delta_{jl}+\delta_{il}\delta_{jk}), \tag{46}$$

which results in

$$\langle T_{ij}T_{ji}\rangle=\frac{2}{3}s^2_{(2)}=\frac{2}{3}(4\pi)^2G^2\overline{\rho}^2\sigma^2_{(0)} \tag{47}$$

(in the following we shall use the notation $\sigma\equiv\sigma_{(0)}$). Let us introduce the important physical quantity ν, the height of the peak density in units of dispersion (the peak height):

$$\nu=\delta_{\rm eq}/\sigma_{\rm eq}(M), \tag{48}$$

where $\sigma_{\rm eq}(M)\equiv\sigma(t_{\rm eq},M)$.

After introduction of these quantities we shall move to calculation of DM particle velocities and core radius. The velocity $\vec{v}(t)$ is given by the sum of the radial velocity $\vec{v}_{\rm rad}$ and an additional velocity $\vec{v}_{\rm tid}$, which will be considered as a small correction caused by tidal forces. The radial velocity will be calculated without tidal interaction taking into account from the equation

$$\frac{d\vec{v}_{\rm rad}}{dt}=-\mathbf{grad}\phi(r), \tag{49}$$

where the spherically symmetric potential $\phi(r)$ is given by the third term in the right hand side (RHS) of Eq. (39). This equation determines the radial motion of the particle, and its solution is given in the parametric form as [44]

$$r=r_s\cos^2\theta, \quad \theta+\frac{1}{2}\sin 2\theta=\frac{2}{3}\left(\frac{5\delta_{\rm eq}}{3}\right)^{3/2}\frac{t-t_s}{t_{\rm eq}}. \tag{50}$$

The moment of maximum clump expansion t_s and the distance $r=r_s$ at this moment are

$$\frac{t_s}{t_{\rm eq}}=\frac{3\pi}{4}\left(\frac{5\delta_{\rm eq}}{3}\right)^{-3/2}, \quad \frac{r_s}{r_{\rm eq}}=\frac{3}{5\delta_{\rm eq}}, \tag{51}$$

where $\delta_{\rm eq}$ is the initial fluctuation value (at $t=t_{\rm eq}$).

Tidal forces give rise to the additional velocity $\vec{v}_{\rm tid}$. Its evolution is described by the equation

$$\frac{dv_{{\rm tid},i}}{dt}=-T_{ij}(t)r^j \tag{52}$$

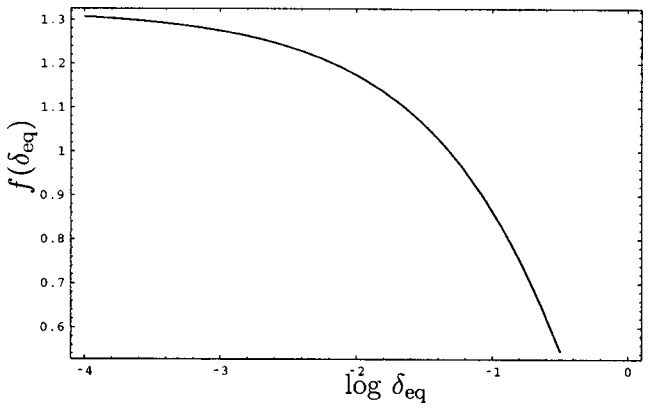

FIG. 1. Function $f(\delta_{eq})$ defined by Eq. (55). The ratio of the core radius to the clump radius in the typical case $\simeq 0.3\nu^{-2} f(\delta_{eq})$.

where in the linear approximation

$$T_{ij}(t) = T_{ij}(t_{eq})\left(\frac{t}{t_{eq}}\right)^{-4/3}. \quad (53)$$

The linear approximation for tidal forces is justified because they are generated by large-scale perturbations which become nonlinear later than the small-scale perturbation under consideration.

Now we find the value $\vec{v}_{tid}$ at the moment when the density nonlinearity sets in, $\delta \simeq 1$, or more exactly at the moment of maximum expansion t_s. After integration of Eq. (52) with the help of Eq. (50) we obtain

$$v_{tid,i}(t_s) = 18^{1/3}\left(\frac{5\delta_{eq}}{3}\right)^{1/2} t_{eq} f(\delta_{eq}) T_{ij}(t_{eq}) r^j(t_s), \quad (54)$$

where the function

$$f(\delta_{eq}) = \frac{2}{3}\int_{(5\delta_{eq}/3)^{1/2}}^{\pi/2} d\phi \left(\phi - \frac{1}{2}\sin 2\phi\right)^{-4/3} \sin^4\phi \quad (55)$$

is plotted in Fig. 1. We may use approximately $f(\delta_{eq}) \simeq 1$ for the values of δ_{eq} of interest [asymptotically $f(\delta_{eq}) \to 1.32$ at $\delta_{eq} \to 0$].

To find the core radius R_c of the clump we shall use a method similar to that in [9]. Since $\mathbf{rot}\vec{v}_{tid} = 0$ and $\mathbf{div}\vec{v}_{tid} = 0$, the tensor T_{ij} has the following diagonal form in the coordinate system connected with the main axes:

$$T'_{ij} = \begin{pmatrix} \tau & & \\ & \tau & \\ & & -2\tau \end{pmatrix}. \quad (56)$$

The value τ from Eq. (56) is connected with the core radius R_c due to the energy relation $\Delta E \simeq \Delta V$, where $\Delta E \simeq \int d^3r\, \rho_{int}(t_s) v_{tid}^2(t_s)/2$ is the work performed by tidal forces, and $\Delta V \simeq GMM_c/R$, where $M_c \sim 4\pi R_c^3 \rho_c/3$, is the potential energy of the core. It gives for the relative core radius

$$x_c \simeq \frac{2^{2/3}3^{10/3}}{\pi}\frac{\tau^2 t_{eq}^2 \delta_{eq}}{G\bar{\rho}_{int}} f^2(\delta_{eq}). \quad (57)$$

From the invariance of the matrix trace relative to the change of coordinates one has

$$\tau^2 = T'_{ij}T'_{ji}/6 = T_{ij}T_{ji}/6. \quad (58)$$

Since the correlator

$$\langle T_{ij}\delta\rangle = \left\langle \left(\Phi_{ij} - \frac{1}{3}\Phi_{ll}\delta_{ij}\right)[\Phi_{ll}(4\pi G\bar{\rho})^{-1} - 1]\right\rangle = 0, \quad (59)$$

the quantities δ and T_{ij} are statistically independent and we may average them independently. Averaging $\langle \tau^2 \rangle$ over the tidal force field T_{ij} with the help of Eqs. (47) and (58), we obtain the main result of this section for the relative core radius:

$$x_c = \frac{R_c}{R} \simeq \frac{\pi 2^{5/3}3^{13/3}}{5^3} G\rho_{eq} t_{eq}^2 \nu^{-2} f^2(\delta_{eq}) \simeq 0.3\nu^{-2} f^2(\delta_{eq}), \quad (60)$$

where ν is given by Eq. (48).

The fluctuations with $\nu \sim 0.5$–0.6 have $x_c \sim 1$, i.e., these fluctuations are practically destroyed by tidal interactions. Most of the galactic clumps are formed from $\nu \sim 1$ peaks. As will be demonstrated in Sec. VI, those clumps that survive until now are characterized by $\nu \simeq 1.6$, but the main contribution to the annihilation signal is given by the clumps with $\nu \simeq 2.5$ for which $x_c \simeq 0.05$.

In an alternative approach for calculation of the core radius, one may define R_c as the minimum deviation of a typical particle trajectory from the center of the clump. After clump virialization a particle at the average distance $R/2$ from the center has an angular momentum $mv_{tid}R/2$. At $t > t_s$ the tidal force is already small and the angular momentum is approximately concerved. Then at the minimum distance from the core R_c, one has $R_c V \sim v_{tid}R/2$, where $V = (2GM/R)^{1/2}$ is the velocity of a typical particle in the center of the virialized clump. Calculating v_{tid} from Eq. (54) and using Eq. (47), one obtains

$$x_c \simeq 0.15\nu^{-1} f(\delta_{eq}), \quad (61)$$

which numerically is very close to Eq. (60) for typical values of $\nu \simeq 1$–3.

The core radius, given by Eq. (60), is much larger than $x_c \simeq \delta_{eq}^3$ obtained in [9] and x_c from [23]. The core radius found in [23] is valid only in a perfectly symmetric case.

Several remarks are in order.

Tidal forces prevent the appearance of singularity during evolution of the clump, but if such a singularity has somehow appeared, tidal interactions cannot destroy it.

In the calculations above we operated with average tidal force, described by Eq. (47). In reality this force fluctuates due to the positions of the surrounding fluctuations, which can overlap with the considered one or be far away from it.

As a result some clumps can be destroyed and those surviving have different core radii R_c. This effect increases the annihilation signal.

We assume that the DM distribution within the core is much flatter than $r^{-\beta}$. Between R_c and the beginning of the asymptotic regime $\rho_{\rm int} \propto r^{-\beta}$ there is a transition zone. During hierarchical evolution (see the next section) this zone expands due to tidal interaction in the hierarchical structures. However, this interaction cannot destroy the existing core.

The above calculations are also valid for the formation of galaxies. It is useful to compare Eq. (60) with observations of galaxies. In [47] the number of peaks in the Gaussian random field is confronted with the observed density of spiral and elliptical galaxies. It was found that these galaxies are formed mostly from peaks with $\nu \simeq 3$. According to Eq. (60) for these peaks $x_c \simeq 0.033$. The rotation curves in the central part of dwarf and low surface brightness galaxies are measured [48,49] and constant-density cores were revealed. Existing observations do not contradict the presence of an extended uniform core with radius $R_c = x_c R \sim 3.3$ kpc in spiral and elliptical galaxies. However, at these distances the baryonic matter dominates, which makes the observation of the DM core even more difficult. The extreme value $R_c = R$ corresponds to $\nu_{\rm min} \approx 0.55 f$. The Gaussian peaks with these ν are completely washed out by tidal forces and do not produce gravitationally bound objects. The intermediate case $\nu \simeq 1$ corresponds to most numerous dwarf and irregular galaxies with the pronounced overdensity in the central core.

V. TIDAL DESTRUCTION OF CLUMPS IN THE HIERARCHICAL MODEL

In this section we shall study the destruction of clumps by the tidal interaction which occurs at the formation of hierarchical structures, but a long time before galaxy formation. This interaction arises when two clumps pass near each other and when a clump moves in the external gravitational field of the bigger object (host) to which this clump belongs. In both cases a clump is exited by the external gravitational field, i.e., its constituent particles obtain additional velocities in the c.m. system. The clump is destroyed if its internal energy increase ΔE exceeds the corresponding total energy $|E| \sim GM^2/2R$. In Sec. V B we shall calculate the rate of excitation energy production due to both aforementioned processes. In Sec. V C we shall calculate the survival probability for a clump in the hierarchical model, in which the smaller clumps are embedded in a bigger one, and the latter enters into a bigger clump, etc. But first we shall describe the necessary generalities and definitions.

A. Generalities and definitions

The formation of DM objects with a fixed mass M at the linear stage is distributed over formation epochs t_f. In the spherical model of the Press-Schechter theory [38,40] the density perturbation at the epoch of object formation is equal to $\delta_c = 3(12\pi)^{2/3}/20 \simeq 1.686$:

$$\delta(M, t_f) = \delta_c \tag{62}$$

Equation (62) gives the *formation criterion* for DM objects. The formation criterion alone does not determine t_f for a given mass M, because $\delta(M)$ has a Gaussian distribution. The formation time t_f can be fixed by an additional condition, e.g., $\nu = 1$ [see Eq. (48)]. The DM objects that satisfy the formation criterion (62) and $\nu = 1$, or equivalently $\sigma(M, t_f) = \delta_c$, will be referred to as *typical* objects. For a given mass M they are characterized by a fixed epoch of formation t_f. In some parts of our consideration we shall simplify the problem, assuming that clumps are *typical* instead of taking into account their distribution over t_f.

We confine ourselves here only to the power-law spectrum of fluctuations $P_{\rm eq}(k) \propto k^n$, in which case

$$\sigma_{\rm eq}(M) \propto M^{-(n+3)/6}. \tag{63}$$

The effective power-law index n obtained from the expression above can be given as

$$n = -3 - 6 \frac{\partial \ln \sigma_{\rm eq}(M)}{\partial \ln M}. \tag{64}$$

In the case of an arbitrary $P(k)$ spectrum, $\sigma_{\rm eq}(M)$ also has an arbitrary dependence on M. Equation (64) defines $n_{\rm eff}$ for some mass interval ΔM. In realistic cases [see, e.g., Eq. (92)], Eq. (64) is a good approximation because the power-law index n depends only weakly on M.

We shall introduce for convenience the characteristic values of typical objects labeled by the index Λ and described by the condition $\sigma(t_\Lambda, M_\Lambda) = \delta_c$ at some fixed moment t_Λ or redshift z_Λ. We can choose these quantities arbitrarily (because they will not enter into the final results), but satisfying the condition $z_\Lambda \gg (\Omega_\Lambda/\Omega_m) - 1$, e.g., taking $z_\Lambda \sim 5-10$. The convenience of these normalizing values is that at $t < t_\Lambda$ the Λ term can be neglected, while small-scale object formation occurs at these epochs. Let us introduce also the dimensionless mass m as

$$m = M/M_\Lambda.$$

Using the formation criterion (62) we obtain

$$\delta(M, t_f) = \delta_{\rm eq} \frac{1+z_{\rm eq}}{1+z_f} = \delta_c \tag{65}$$

because the growth factor for the rising mode $D_g(t) \propto (1+z) \propto t^{2/3}$ in the standard cosmological model at the matter-dominated epoch. For a single clump with mass M obeying $\delta_{\rm eq} = \nu \sigma_{\rm eq}(M)$ with an arbitrary ν one has

$$\overline{\rho}_{\rm int} = \kappa \overline{\rho}(z_f) = \kappa \rho_{\rm eq} \left(\frac{1+z_{\rm eq}}{1+z_f} \right)^3 = \kappa \rho_{\rm eq} \frac{\nu^3 \sigma_{\rm eq}^3(M)}{\delta_c^3}, \tag{66}$$

and

$$R = \left(\frac{3M}{4\pi \overline{\rho}_{\rm int}} \right)^{1/3} = \nu^{-1} R_\Lambda m^{(n+5)/6}, \tag{67}$$

where M and R are, respectively, the mass and radius of the clump, $\kappa = 18\pi^2 \simeq 178$ and $R_\Lambda = [3M/4\pi\kappa\overline{\rho}(t_\Lambda)]^{1/3}$. The

value of κ describes the increasing clump density during contraction and it can be found from Eq. (50) (see also [40]).

The number density of unconfined (free) clumps (i.e., of those not belonging to the more massive objects) is given by the Press-Schechter formulas [40]

$$\phi_{\rm PS}(t,M)dM = \left(\frac{2}{\pi}\right)^{1/2}\frac{\rho}{M}\frac{\delta_c}{D_g(t)\sigma_{\rm eq}^2}\frac{d\sigma_{\rm eq}}{dM}\exp\left[-\frac{\delta_c^2}{2D_g(t)^2\sigma_{\rm eq}^2}\right]dM, \tag{68}$$

where the growth factor $D_g(t)$ is normalized as $D_g(t_{\rm eq})=1$. Let us consider the Press-Schechter distribution for the clumps hosted by the larger clump at the moment t_f of its formation. Taking into account the density increase factor κ we obtain

$$\psi_{\rm PS}(t_f,m)dm=\kappa\phi_{\rm PS}(t_f,m)dm. \tag{69}$$

As will be demonstrated in this section the clumps are destroyed by tidal interaction and each clump has a small survival probability $\xi<0.01$. A surviving clump during its lifetime is surrounded by other clumps with a distribution given by Eq. (69). When a host clump is destroyed, the surviving clump finds itself hosted by a larger clump with the small clump distribution inside given by the same Eq. (69) but with larger t_f. Since the tidal destruction is most effective at small distances, one should always consider the smallest possible host clump of the hierarchical structure, and the distribution of the small clumps around the one under consideration is always given by Eq. (69). The characteristic time is the time of formation t_f of the smallest host clump, although the time of destruction can be much larger than t_f.

The total energy (kinetic and potential) of a clump is given by

$$|E|=\frac{3-\beta}{2(5-2\beta)}\frac{GM^2}{R}. \tag{70}$$

B. The rate of internal energy growth

Consider a host clump with mass M_h and radius R_h, and with the small clumps inside having the distribution (69) and moving in the common gravitational potential with a velocity dispersion $\sim V_h\simeq GM_h/R_h$. Interacting tidally with its neighbors, a small clump increases its internal energy. We calculate first the rate of internal energy increase due to these interactions. The mass of the considered clump is $M=mM_\Lambda$, it is characterized by an arbitrary ν, and its interaction with a target clump occurs at the impact parameter l. The target clump is characterized by a mass M', radius R', radius of the core $R_c'=x_cR$ with $x_c\sim0.1$, and universal density distribution (3).

The increase of internal energy of a clump M during one flyby in the momentum approximation [50] is given by

$$\Delta E=\frac{1}{2}\int d^3r\,\rho(r)(v_x-\tilde{v}_x)^2, \tag{71}$$

where v_x is the velocity *increase* of DM particles in the direction of the axis x, and $\tilde{v}_x$ is the same for the c.m. of the clump. The axis x connects the c.m.'s of two clumps when the distance between them is the shortest. One has approximately

$$v_x-\tilde{v}_x\simeq\frac{\partial v_x}{\partial l}\Delta l=\frac{\partial v_x}{\partial l}r\cos\psi, \tag{72}$$

where ψ is the polar angle in spherical coordinates.

For nearly straightforward propagation, the angle between $\vec{v}_{\rm rel}$ and the line connecting c.m.'s of the clumps evolves as

$$\frac{d\phi}{dt}=-\frac{v_{\rm rel}}{l}\cos^2\phi, \tag{73}$$

where $v_{\rm rel}\simeq\sqrt{2}V_h$. Changing the variable t to ϕ in the Newton equation one gets

$$\frac{dv_x}{d\phi}=-\frac{GM'[r'(\phi)]}{v_{\rm rel}l}\cos\phi, \tag{74}$$

and after integration of this equation

$$v_x=\frac{2GM'}{v_{\rm rel}R'}g(y), \tag{75}$$

where $y=l/R'$,

$$g(y)=\begin{cases} y^{-1}, & y>1,\\ \left[1+y^{3-\beta}(1-y^2)^{1/2}\,{}_2F_1\left(\frac{3-\beta}{2},\frac{1}{2},\frac{3}{2},1-y^2\right)\right. & \\ \qquad\left.-(1-y^2)^{1/2}\right]/y, & y<1, \end{cases} \tag{76}$$

and ${}_2F_1$ is the hypergeometric function.

The rate of internal energy growth due to collisions with all other clumps is

$$\dot{E}=\int 2\pi l v_{\rm rel}dl\int dM'\psi(M',t)\Delta E. \tag{77}$$

After simple calculations, one obtains

$$\dot{E}=\frac{4\pi(3-\beta)}{3(5-\beta)}\frac{G^2MR^2}{v_{\rm rel}}\int_M^{M_h}dM'M'^2\psi(M',t) \times\left[\frac{\lambda}{R'^2}+\frac{1}{2}\left(\frac{1}{R'^2}-\frac{1}{R_h^2}\right)\right], \tag{78}$$

where

$$\lambda=\int_{x_c'}^1 dy\,y\left(\frac{dg}{dy}\right)^2=0.11 \tag{79}$$

for $x_c'=0.1$ and the dependence of λ on x_c' is very weak.

As the second process of tidal destruction, we shall consider the interaction with the common gravitational potential

of a host clump. The energy gain per mass unit at a distance r from the c.m. of the considered small clump m during one periastron passage [50] is

$$\langle E_p\rangle = \frac{GM_h}{R_h^3} r^2 \left(\frac{R_h}{R_p}\right)^{\beta} \chi_{\rm ecc}(e) A(\omega\tau), \tag{80}$$

where e is the eccentricity, the function $\chi_{\rm ecc}$ is presented in [50], the adiabatic correction $A(x)=(1+x^2)^{-\gamma}$, $\gamma\simeq 2.5-3$, and R_p is the periastron separation. The energy gain of a clump during one period $T_{\rm orb}$ is $\Delta E=\int\langle E_p\rangle\rho_{\rm int}(r)d^3r$, and the rate of energy growth is

$$\dot{E}=\frac{2\Delta E}{T_{\rm orb}}. \tag{81}$$

The rate of energy growth due to both of the aforementioned processes is given by the sum of Eqs. (78) and (81). Using the distribution (69) in the integral of (78) and the total energy of a clump given by Eq. (70), we find

$$\frac{1}{T(m,m_h,\nu,\nu_h)}\equiv\frac{\dot{E}}{E}\simeq 2t_\Lambda^{-1}\mu\nu_h^{9/2}\nu^{-3}m^{(n+3)/2}m_h^{-3(n+3)/4}, \tag{82}$$

where

$$\mu=\frac{2^{1/2}\kappa^{1/2}(5-2\beta)}{3(5-\beta)}\left[\left(\frac{R_h}{R_p}\right)^{\beta}A(\omega\tau)\chi_{\rm ecc}(e) + \frac{1}{4\pi^{1/2}}\left|\frac{n+3}{n+1}\right|\left(2\lambda+\frac{n+5}{n+9}\right)\right]. \tag{83}$$

The first term in the square brackets describes the interaction with the common gravitational field of the host clump, while the second term describes ''collisions'' with small clumps inside the host clump. Usually the former is larger than the latter. For calculations we shall consider an average orbit with $R_h/R_p\simeq 2$ and $T_{\rm orb}\simeq 2R_h/V_h$, and put $A(\omega\tau)\chi_{\rm ecc}(e)\sim 1$. If we neglect the tidal interactions with the small clumps [the second term in the square brackets in Eq. (83)] and use $\beta=1.8$, one has $\mu\simeq 9.6$. The dependence of our final result (mass function of the clumps) on μ is weak, going approximately as $\mu^{-1/3}$.

C. Survival probability in the hierarchical model

A small clump with mass m during its lifetime can be a constituent part of many host clumps of successively larger masses m' and virial velocities V'. After tidal disruption of the lightest host, a small clump automatically becomes a constituent part of the heavier host, etc. Transition of a small clump from one host to another occurs almost continuously in time up to formation of a host where tidal destruction becomes inefficient. The fraction of small clumps with mass m escaping the tidal destruction is given by e^{-J}, with

$$J\simeq\sum_{m'}\frac{\Delta t}{T(m,m',\nu,\nu')}, \tag{84}$$

where the summation goes over the intermediate big clumps which successively host the small clump m, and Δt approximately equals the difference of formation times of two successive hosts.

Let us introduce the notation: m_1 is the mass of the first (lightest) host clump which contains the considered light clump m, and m_n is the last such object, e.g., the Galactic halo. A formation epoch for the host clump m' is

$$t_f(m',\nu')=t_\Lambda\left(\frac{1+z'}{1+z_\Lambda}\right)^{-3/2}=t_\Lambda m'^{(n+3)/4}\nu'^{-3/2}. \tag{85}$$

Note that J does not depend on t_Λ since it enters linearly in t_f and in T as seen from Eq. (82).

The first host gives a major contribution to the clump destruction, especially if its mass m_1 is close to m and $\nu_1\simeq\nu$. For the considered clump m and for the first two hosts $\sigma_{\rm eq}(M)\simeq\sigma_{\rm eq}(M_1)\simeq\sigma_{\rm eq}(M_2)$ because $\sigma_{\rm eq}(M)$ depends weakly on M according to Eq. (64). The considered clump m and the first two hosts differ mainly in their masses and in the values of ν ($\nu\geqslant\nu_1\geqslant\nu_2$). It justifies the following simplification: we consider all hosts beginning from the second one as typical objects ($\nu_i=1$ for $i=2,3,...$) and, separating the first term in the sum (84), substitute the remaining sum by the integral.

$$J\simeq\frac{t_f(m_2,\nu_2=1)-t_f(m_1,\nu_1)}{T(m,m_1,\nu,\nu_1)} + \int_{m_2}^{m_n}\frac{1}{T(m,m',\nu,\nu'=1)}\frac{dt_f(m',\nu'=1)}{dm'}dm'. \tag{86}$$

We may now change the lower limit m_2 to m_1 in the above integral because it depends on m_2 weakly, only through $m_2^{(n+3)/2}$ with $(n+3)/2\ll 1$, where n is given by Eq. (64). In addition we may put the upper limit $m_n\to\infty$ without loss of accuracy. Inserting Eq. (82) into Eq. (86) we finally obtain the following approximate expression for J:

$$J\simeq 2\mu\frac{\nu_1^{9/2}}{\nu^3}\left(\frac{m}{m_1}\right)^{(n+3)/2}(1-\nu_1^{-3/2})\theta(\nu_1-1) + \mu\nu^{-3}\left(\frac{m}{m_1}\right)^{(n+3)/2}, \tag{87}$$

where the step function $\theta(x)=1$ for $x>0$ and 0 for $x\leqslant 0$. In the case of $\nu_1=1$ the formation moment of the first host almost coincides with the formation moment of the second one, for which $\nu_2=1$ in the approach used.

The differential fraction of mass in the form of clumps which escape tidal destruction in the hierarchical objects can be found as

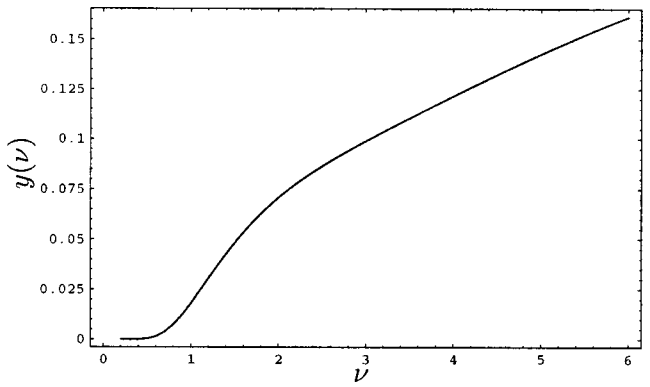

FIG. 2. Function $y(\nu)$ from Eq. (90) obtained by the numerical integration of Eq. (88). This curve is valid with good accuracy for all β from the interval $1 \leqslant \beta \leqslant 2$.

$$\xi(n,\nu)\frac{dm}{m}d\nu = dm\, d\nu (2/\pi) e^{-\nu^2/2} \int_0^{\nu} d\nu_1 e^{-\nu_1^2/2} \times \int_{t_f(m,\nu)}^{\infty} dt_1 \left| \frac{\partial^2 F(m,t_1)}{\partial m \partial t_1} \right| e^{-J}, \quad (88)$$

where the variable m_1 in J is connected with t_1 and ν_1 according to Eq. (85), $F(m,t)$ is the mass fraction of unconfined clumps with masses smaller than m at the moment t, which according to [40] is given by

$$F(m,t) = \mathrm{erf}\left\{ \frac{\delta_c}{\sqrt{2}\sigma_{\mathrm{eq}}(M) D_g(t)} \right\}. \quad (89)$$

Here $\mathrm{erf}(x)$ is the error integral and $D_g(t)$ is the growth factor. After numerical calculations for $\beta = 1.8$ we finally obtain

$$\xi(n,\nu) \simeq (2\pi)^{-1/2} e^{-\nu^2/2} (n+3) y(\nu), \quad (90)$$

where the function $y(\nu)$ is plotted in Fig. 2. It depends weakly on β.

This is the main result of this section. We shall refer to ξ as to the *clump survival probability*.

Our final result, the distribution of surviving clumps over their masses M and ν, which for fixed M determines the clump radius R, is given by $\xi(n,\nu) d\nu\, dM/M$, where ξ depends very weakly on M only through the weak dependence of $n(M)$ [see Eq. (64)]. For the most numerous clumps with $\nu = 1$ and for the unit intervals $d\nu$ and $d \ln M$, ξ has the meaning of the fraction of the DM mass in the form of clumps relative to free DM particles, as introduced in Eq. (10). By integrating over ν, we obtain

$$\xi_{\mathrm{int}} \simeq 0.01(n+3). \quad (91)$$

This means that, for different n, about 0.1–0.5% of clumps survive the stage of tidal destruction in each logarithmic mass interval $\Delta \ln M \sim 1$.

Several remarks are in order.

The physical meaning of the surviving clump distribution $\xi(n,\nu) d\nu\, dM/M$ is different from that for unconfined (free) clumps given by the Press-Schechter mass function $\partial F/\partial m$. The surviving clump distribution implies that each DM particle belongs simultaneously to several host clumps put into each other, and for this reason the integral $\int \xi\, dm/m$ is divergent.

To calculate ξ we need to know the power-law index n in the perturbation spectrum, which can be taken as n_{eff} from Eq. (64) for a given $\sigma_{\mathrm{eq}}(M)$. To find the latter, the primeval (e.g., inflation) power spectrum of the fluctuations is needed. The simplest inflation models give $P_p(k) \propto k^{n_p}$ with $n_p \approx 1$. The analysis of the WMAP measurement of the cosmic microwave background (CMB) anisotropy [51] gives a power-law spectrum with $n_p = 0.99 \pm 0.04$ in good agreement with $n_p = 1$. However, when data from the galaxy power spectrum with two degrees of freedom and *Ly-α* are included in analysis, the best-fit favors a mild tilt, $n_p = 0.96 \pm 0.02$.

The variance $\sigma_{\mathrm{eq}}(M) = \sigma_{(0)}$ from Eq. (44) in the small-scale range is found in [52] (see also [53]). We present this result as

$$\sigma_{\mathrm{eq}}(M) \simeq \frac{2\times 10^{-4}}{\sqrt{f_s(\Omega_\Lambda)}} \left[\ln\left(\frac{k}{k_{\mathrm{eq}}} \right) \right]^{3/2} \left(\frac{k}{k_{h0}} \right)^{(n_p-1)/2} \simeq 8.2\times 10^{3.7(n_p-1)-3} \left[1 - 0.06 \log\left(\frac{M}{M_\odot} \right) \right]^{3/2} \times \left(\frac{M}{M_\odot} \right)^{(1-n_p)/6}, \quad (92)$$

where k_{eq} and k_{h0} correspond to the mass inside the cosmological horizon at the moments t_{eq} and t_0, respectively, and

$$f_s(\Omega_\Lambda) = 1.04 - 0.82\Omega_\Lambda + 2\Omega_\Lambda^2 \quad (93)$$

according to [52]. We used above the relation $k \propto M^{-1/3}$ and the values

$$M_{\mathrm{eq}} = 1.5\times 10^{49} \Omega_m^{-2} h^{-4}\ \mathrm{g}, \quad M_{h0} = 6\times 10^{55} \Omega_m h^{-1}\ \mathrm{g}. \quad (94)$$

Using the power-law spectrum of fluctuations down to small scales, while normalization by the CMB anisotropy is performed at a large scale, implies an extrapolation of the spectrum by many orders of magnitude. Such extrapolation is justified only by the confidence in inflation models which predict the power-law spectrum valid for many orders of mass magnitude.

It is interesting to note that the differential number density of clumps in the Galactic halo $n(M) dM \propto dM/M^2$, obtained from Eq. (90), is very close (including the normalization coefficient) to that obtained in the numerical simulations for clumps with large masses $M \geqslant 10^8 M_\odot$ [$n(M) dM \propto dM/M^{1.9}$ [4]]. Strictly speaking, our calculations are not valid for clumps with these masses, because of their destruction in the halo up to the present epoch t_0 and accretion of new clumps onto the halo. Nevertheless, for the small interval of masses where the power-law spectrum can be used as a rather good approximation, our approach can be roughly valid.

VI. NUMERICAL RESULTS

In this section we shall present the numerical results of our calculations: the enhancement factor for the annihilation signal, the distribution of DM clumps over their masses M and radii R, and the distribution of clumps in the Galactic halo.

Using Eqs. (6) and (7) we find the enhancement of the annihilation signal due to clumpiness of the halo as the generalization of Eq. (10) for the clumps distributed over M and R:

$$\eta(M_{\min},n_p) = 1+\frac{1}{\tilde{\rho}_{\rm DM}}\int_{\nu_{\min}}^{\infty} d\nu \int_{M_{\min}} \frac{dM}{M} S[\beta,x_c(\nu)]\xi\overline{\rho}_{\rm int}(M,\nu), \tag{95}$$

where

$$\xi=\xi(n,\nu) \tag{96}$$

is defined by Eq. (90), the effective spectrum index $n(M,n_p)$ is calculated from Eq. (64) for the primeval (inflation) spectrum index n_p, with $\sigma_{\rm eff}(M)$ taken in the form (92); $\overline{\rho}_{\rm int}$ is given by Eq. (66) and $\nu_{\min}\simeq 0.55$. The function S is taken in the form (4), which corresponds to the density profile (3), and we used Eq. (60) for the clump virial radius R.

Most of the surviving clumps are formed from fluctuations with a mean value of the peak height

$$\langle\nu\rangle \simeq \frac{\int d\nu\, \nu e^{-\nu^2/2} y(\nu)}{\int d\nu\, e^{-\nu^2/2} y(\nu)} \simeq 1.6. \tag{97}$$

Meanwhile, the main contribution to the enhancement of the annihilation signal (95) comes from the clumps with an effective value of the peak height

$$\langle\nu\rangle_{\rm ann} \simeq \frac{\int\int d\nu\, \nu S\xi\overline{\rho}_{\rm int} dM/M}{\int\int d\nu\, S\xi\overline{\rho}_{\rm int} dM/M} \simeq 2.5 \tag{98}$$

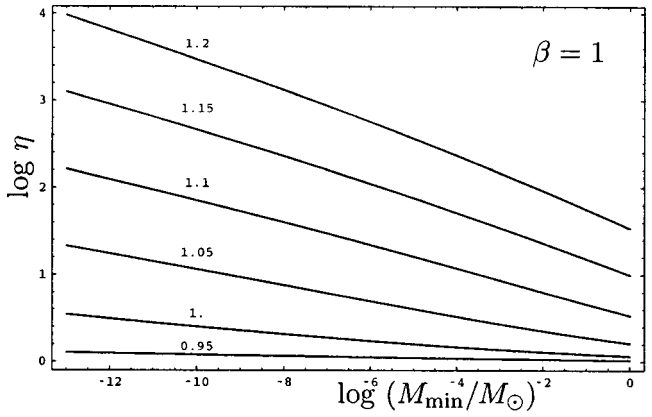

FIG. 3. The global enhancement η of the annihilation signal from Eq. (95) as a function of the minimal clump mass $M_{\min}$, for a clump density profile with index $\beta=1$ and for different indices n_p of the primeval perturbation spectrum. The curves are marked by the values of n_p.

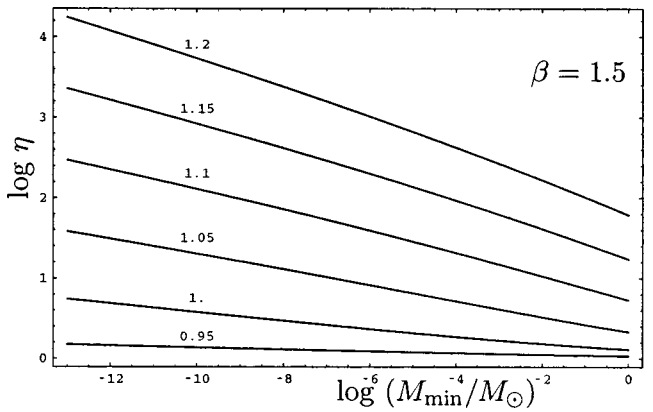

FIG. 4. The same as Fig. 3 but for $\beta=1.5$.

for $\beta=1.8$. The clumps with $\nu\simeq 2.5$ have $x_c\simeq 0.05$.

For the Galactic halo we use the Navarro-Frenk-White (NFW) density profile [10]

$$\rho_{\rm DM}(l)=\frac{\rho_0}{(l/L)(1+l/L)^2}, \tag{99}$$

with $L=45$ kpc according to [54], and ρ_0 fixed by the local density value $\rho_{\rm DM}(r_\odot)=0.3\ {\rm GeV\,cm^{-3}}$. With these parameters the halo mass within the virial radius of 100 kpc is $10^{12}M_\odot$. Equation (9) gives $\tilde{\rho}_H=1.02\rho_H(r_\odot)$, i.e., these values practically coincide.

The values of global enhancement $\eta(M_{\min},n_p)$ as given by Eq. (95) are displayed in Figs. 3–5 for different values of $M_{\min}$, β, and n_p. As a representative example consider the clump with the Gurevich-Zybin [9] density profile with $\beta=1.8$ (see Fig. 5): numerically $\eta=5$ for $M_{\min}=2\times10^{-8}M_\odot$ and $n_p=1.0$. It strongly increases at smaller $M_{\min}$ and larger n_p. For example, for $n_p=1.1$ and 1.2 at the same $M_{\min}=2\times10^{-8}M_\odot$, the enhancement becomes tremendously large, $\eta=130$ and 4×10^3, respectively.

Our approach is based on the hierarchical clustering model in which smaller-mass objects are formed earlier than larger ones, i.e., $\sigma_{\rm eq}(M)$ diminishes with the growth of M. This condition is satisfied for objects with mass $M>M_{\min}\simeq 2\times10^{-8}M_\odot$ only if the primordial power spectrum has the

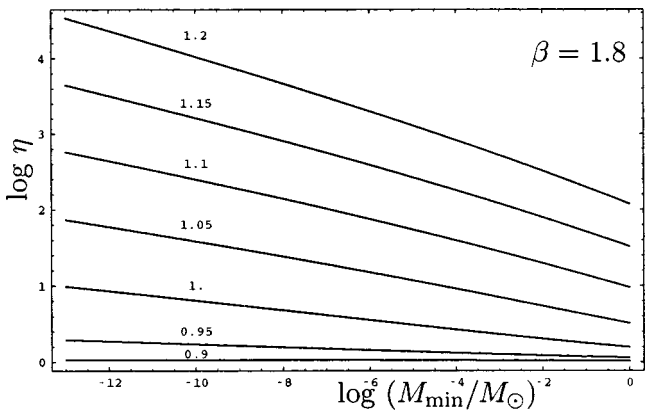

FIG. 5. The same as Fig. 3 but for $\beta=1.8$.

value of the power index $n_p > 0.84$. As seen from Figs. 3–5, in this case the enhancement of the annihilation signal in fact is absent, $\eta \simeq 1$, for $n_p < 0.9$.

We discussed above the global enhancement of the annihilation signal. In fact the enhancement varies in different directions relative to the Galactic center (GC). It can easily be seen from Eqs. (6) and (7), which show that while $I_{\rm cl}$ is proportional to $n_{\rm cl}(l)$ [and thus to $\rho_{\rm DM}(l)$ everywhere except the core], $I_{\rm hom}$ is proportional to $\rho^2_{\rm DM}(l)$. This implies that the relative contribution of $I_{\rm hom}$ increases in the directions close to the GC where $\rho_{\rm DM}(l)$ is larger. This effect is further enhanced by the destruction of the clumps in the core around the GC. Our numerical calculations confirm this expectation: the ratio of enhancement in the directions to the GC and anticenter is 0.2 for a NFW density profile and for the core radius of 3 kpc. Therefore, the presence of the clumps diminishes the anisotropy of the annihilation signal, caused by the density profile of DM in the halo.

Our results suffer from uncertainties in the input parameters. As was mentioned above $\tilde{\rho}_{\rm DM} \simeq \rho_{\rm DM}(r_\odot)$. It remains approximately true not only for the NFW density profile but also for other profiles discussed in the literature. For example, for an isothermal profile with the core radius 10 kpc, $\tilde{\rho}_{\rm DM} = 0.65 \rho_{\rm DM}(r_\odot)$. Another uncertainty in the value of η is imposed by the value of $\rho_{\rm DM}(r_\odot)$. According to different estimates $\rho_{\rm DM}(r_\odot) = 0.2 - 0.6\ {\rm GeV\,cm^{-3}}$. The corresponding uncertainty in η is given by a factor of 0.5–1.5.

For illustration, we shall numerically describe the properties of the clumps which give the main contribution to the annihilation rate. Basically, they are those with $M \sim M_{\rm min}$ and $\nu \sim \langle \nu \rangle$. The rms fluctuation values $\sigma_{\rm eq}(M)$ for clumps with minimal mass $M_{\rm min} \simeq 2 \times 10^{-8} M_\odot$ and for $n_p = 1$ and 1.2 are $\sigma_{\rm eq} = 0.015$ and 0.14, respectively, according to Eq. (92). From Eq. (98) the effective value of $\nu = \delta_{\rm eq}/\sigma_{\rm eq}$ is $\langle \nu \rangle \simeq 2.5$. From Eqs. (66) and (67) it follows that clumps with this ν are characterized by the density and radius $\overline{\rho}_{\rm int} \simeq 2 \times 10^{-22}\ {\rm g\,cm^{-3}}$, $R \simeq 3.6 \times 10^{15}$ cm and $\overline{\rho}_{\rm int} \simeq 2 \times 10^{-19}\ {\rm g\,cm^{-3}}$, $R \simeq 3.7 \times 10^{14}$ cm for $n_p = 1$ and 1.2, respectively. The part of the Galactic halo mass in the form of these clumps is of the order of $\xi_{\rm int} \sim 0.002$ according to Eq. (91). The mean number density of the clumps in the halo is $\sim 25\ {\rm pc^{-3}}$.

We have given above the characteristic values for the clumps with the dominant contribution to the annihilation signal. The general distribution of clumps in the Galactic halo can be readily calculated numerically from Eq. (90), changing (for given M) the distribution over ν by that over dR:

$$n_{\rm cl}(M,R)\, d\ln M\, d\ln R = \frac{\rho_{\rm DM}(r_\odot)}{M}\, \xi(M,\nu)\, d\ln M\, d\nu. \tag{100}$$

Note that the definition of the clump number density $n_{\rm cl}$ here does not coincide with the similar one in Eq. (5) where dN is given per dR and dM.

The distribution $M n_{\rm cl}(M,R)$ is presented in Fig. 6 as a function of R for different M and for a distance 8.5 kpc from the Galactic center.

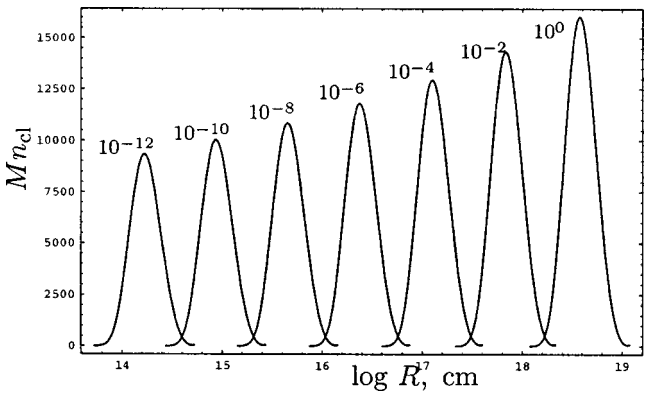

FIG. 6. The mass density of clumps in the Galactic halo $M n_{\rm cl}(M,R)$ in units of $M_\odot/{\rm kpc}^3$, from Eq. (100), as a function of their radius R at the distance 8.5 kpc from the Galactic center for $n_p = 1.0$. The curves are labeled by the values of the clump masses in $M_\odot$

The radius of a clump R in the most general case is determined by M and ν. Due to the weak dependence of $\sigma_{\rm eq}(M)$ on M, the radius of the clump $R(M)$ with sufficiently good accuracy is proportional to $M^{1/3}$. From Eqs. (66) and (67) we have

$$R \simeq 1.5 \times 10^{16} \left(\frac{M}{10^{-6} M_\odot} \right)^{1/3} \left(\frac{\nu}{2.5} \right)^{-1}\ {\rm cm}, \tag{101}$$

for $n_p = 1.0$. For $n_p = 1.1$ the numerical factor in Eq. (101) is 5.5×10^{15} cm.

How are clumps distributed in the Galactic halo? One may expect that this distribution is the same as the distribution of the free DM particles in the halo. This is true for large distances l from the Galactic center, while at small l the tidal interaction with stars results in the destruction of small clumps and in the formation of a core with radius L_c in the clump distribution. The destruction of a clump propagating in the space filled by stars has been studied in [9]. The destruction is important only for clumps inside the bulge, i.e., at a distance $l \leqslant 3$ kpc from the Galactic center. Clumps outside the bulge at distances $3 \leqslant l \leqslant 10$ kpc can interact tidally with stars in the disk. But the time of crossing the disk is very small (in comparison with orbital period) and this process is not important.

The number density of clumps outside the bulge is proportional to the halo density, e.g., to $\xi \rho_{\rm DM}(l)$ in the case of the NFW distribution given by Eq. (99), or can be obtained from Eq. (99) and Fig. 6 by simple scaling.

The density distribution for stars in the bulge according to [55] is given by

$$\rho_s(l) = \begin{cases} \tilde{\rho}(l/\tilde{r})^{-1.8}, & l < \tilde{r}, \\ \tilde{\rho}(l/\tilde{r})^{-3}, & l > \tilde{r}, \end{cases} \tag{102}$$

where $\tilde{\rho} = 1.8 M_\odot/{\rm pc}^3$ and $\tilde{r} = 800$ pc. From Eq. (46) of [2] by substituting Eq. (102) we obtain that inside the bulge ($l \leqslant 3$ kpc), the clumps with $M \leqslant 10^{-4} M_\odot$ are destroyed during the Hubble time. Thus, for these masses the core radius L_c coincides with the size of the bulge $L_{\rm bulge} \simeq 3$ kpc.

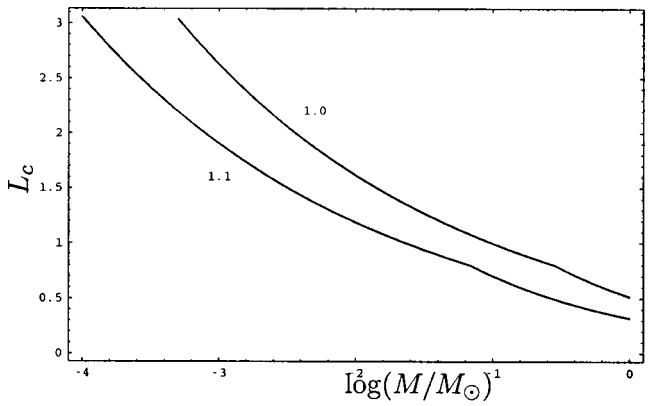

FIG. 7. The radius L_c of the Galactic core (in kpc) in the distribution of clumps with masses M for $n_p=1.0$ and 1.1 in the case $\nu=2.5$.

Clumps with $M \geqslant 10^{-4} M_\odot$ are destroyed during the Hubble time within distances from the Galactic center shown in Fig. 7 for $n_p=1.0$ and 1.1 and $\nu=2.5$. This distance defines the radius of the core L_c for clumps of the given mass M.

Our calculations for enhancement of the annihilation signal disagree with those in [16,27,28].

In [16] the singularity in the Galactic center is cut at a very small core radius, which results in too strong an annihilation signal. According to our calculations the radius of the core is much larger, and the distribution of the clumps in the halo also has a core.

In [27,28] a large enhancement of the signal is found for heavy clumps with $M > 10^6 M_\odot$ [27] and $M > 10^2 M_\odot$ [28]. If it were true, the total signal from clumps with $M \geqslant M_{\min}$ would be too large. A too small core radius was used in these calculations, too.

VII. CONCLUSIONS

We have calculated the number density of the small-scale clumps in the Galactic halo and their distribution over masses M, radii R, and distances to the Galactic center in the framework of the standard cosmological model with the primeval density perturbation $P(k) \propto k^{n_p}$ taken from the inflation models with $n_p \simeq 1$ (the Harrison-Zeldovich spectrum). The most important element of our calculations is inclusion of the tidal interactions, which result in the formation of the clump core and destruction of small-scale clumps.

We consider the most conservative case of the Gaussian adiabatic fluctuations which enter the nonlinear stage of evolution, $t_{\rm nl}$, at the matter-dominated epoch $t_{\rm nl} > t_{\rm eq}$, where $t_{\rm eq}$ is the moment of equality. The time of small-scale clump formation t_f for a clump with mass M is given by two equations: the formation criterion $\delta(M,t_f)=\delta_c$ and the height of the peak density of a fluctuation in units of dispersion $\nu = \delta_{\rm eq}/\sigma_{\rm eq}(M)$, taken at the epoch $t_{\rm eq}$ [see Eqs. (48) and (62) for explanation and notation]. All the processes we are interested in take place at $t \geqslant t_{\rm eq}$ at the stage of nonlinear evolution. We study the growth of fluctuations in the nonlinear regime in the framework of the Press-Schechter theory of hierarchical clustering with the tidal interactions included as the new element. The picture of hierarchical clustering and clump destruction can be described in the following way. Clumps of minimal mass are formed first. A clump of larger mass, which hosts the smaller clumps, is formed later. A bigger clump, which includes the hosts considered with their content, is formed later, etc. The clumps are destroyed in tidal interactions with other small clumps and by the gravitational field of a host clump, with the former process being subdominant. The calculated mass density of the surviving clumps, $\xi(M,\nu)d\nu\, dM/M$, with mass M and ν, is given by Eq. (90), with the survival probability being typically $\xi \sim 0.001-0.005$. The clump number density in the Galactic halo $n_{\rm cl}(M,R)$ for the clumps with mass M and radius R is shown in Fig. 6. These clumps are distributed in the Galactic halo as a function of the distance to the Galactic center l. At large distances the distribution must be the same as found in the numerical simulations (e.g., the NFW profile). At small distances there is a core produced by tidal interaction of the clumps with the stars in the bulge. The radius of the core, L_c, is given in Fig. 7 at $M \geqslant 10^{-4} M_\odot$, and it is equal to the radius of the bulge $L_c \sim 3$ kpc for smaller clump masses.

The mass spectrum of the clumps is characterized by a cutoff at $M_{\min}$. Its value depends on the properties of the DM particle, and thus it is model dependent. The existing calculations of $M_{\min}$ differ drastically: from $M_{\min} \sim 10^{-12}\, M_\odot$ [42] to $M_{\min} \sim 10^{-7}\, M_\odot$ [43].

Cold dark matter particles at high temperature $T > T_f \sim 0.05 m_\chi$ are in thermodynamical (chemical) equilibrium with the cosmic plasma, when their number density is determined by temperature. After decoupling at $t > t_f$ and $T < T_f$, the DM particles remain for some time in kinetic equilibrium with the plasma, when the temperature of the CDM particles T_χ is equal to the temperature of the plasma T, but the number density n_χ is not Planckian any more. At this stage the CDM particles are not perfectly coupled to the cosmic plasma. Collisions between a CDM particle and fast particles of ambient plasma result in the exchange of momentum and a CDM particle diffuses in space. Due to diffusion, the DM particles leak from the small-scale fluctuations, and thus their distribution has a cutoff at minimal mass M_D. The diffusion coefficient is determined by the elastic scattering of DM particles off the plasma particles. Our calculations, made for the neutralino, for which we have chosen the pure B-ino state, give

$$M_D = 4.3 \times 10^{-13} \left(\frac{m_\chi}{100\ {\rm GeV}} \right)^{-15/8} \left(\frac{\tilde{M}}{1\ {\rm TeV}} \right)^{-3/2} M_\odot , \tag{103}$$

where m_χ is the neutralino mass and $\tilde{M}$ is (approximately) the mass of the sneutrino and selectron, which are assumed to be equal. The functional dependence of Eq. (25) and numerical value of Eq. (26) obtained in the diffusion approximation coincide with the corresponding results obtained by a different method in [42].

When the energy relaxation time for DM particles, $\tau_{\rm rel}$, becomes larger than the Hubble time $H^{-1}(t)$, DM particles get out of kinetic equilibrium. This condition determines the

time of kinetic decoupling t_d. At $t \geqslant t_d$ CDM particles are moving in the free streaming regime and all fluctuations on the free streaming scale $\lambda_{\rm fs}$ and smaller are washed out. In contrast to [43], we have calculated the free streaming length $\lambda_{\rm fs}$ taking into account the distribution of neutralino (B-ino) velocities over absolute values and angles from radial directions. The cosmological expansion in the vicinity of $t_{\rm eq}$ is taken exactly, without the usual step-function approximation. Our value of $M_{\rm min}$ due to the free streaming effect is

$$M_{\rm min} = 1.5 \times 10^{-8} \left(\frac{m_\chi}{100 \ \ {\rm GeV}} \right)^{-15/8} \left(\frac{\tilde{M}}{1 \ \ {\rm TeV}} \right)^{-3/2} M_\odot ; \tag{104}$$

see Eq. (38) for more parameters involved.

When normalized to the same masses of neutralino and slepton, our value of $M_{\rm min}$ coincides only within an order of magnitude with [43].

The evolution of a density fluctuation in the nonlinear regime results in the density profile of a clump. The analytic theory of this phenomenon was developed by Gurevich and Zybin (for a review, see [9]); for the numerical simulations see [3,10]. The initial single-stream flow leads to formation of the initial singularity. In contrast to energy-dissipating matter (e.g., baryons), in the flow of nondissipative matter the multistream instability develops [9], when at one point several streams with different radial velocities exist. The surfaces with different numbers of streams are separated by caustics, whose number increases rapidly toward the center. The matter is gravitationally captured in such a structure. A density singularity is produced in the center, unless additional phenomena are included in consideration. Of these, the interaction with the damped mode [9] and annihilation of DM particles [23] were previously studied. We have demonstrated here that tidal forces due to the external gravitational field cause the deflection of DM particles from radial motion, and thus prevent the formation of a singularity. The core produced has a radius R_c given in the approximate form as

$$x_c = \frac{R_c}{R} \simeq 0.3 \nu^{-2}, \tag{105}$$

[see Eq. (60) for the exact expression and the discussion afterward]. This radius is much bigger than those obtained in [9,23].

The majority of clumps are formed from $\nu \sim 1$ peaks, while the surviving clumps are characterized on average by $\nu \simeq 1.6$. The clumps which give the dominant contribution to the annihilation signal have $\nu \simeq 2.5$.

In spite of the small survival probability $\xi \sim 0.1$–$0.5\,\%$, clumps in most cases provide the dominant contribution to the annihilation rate in the halo. The enhancement of the annihilation signal can be characterized by the ratio $\eta = (I_{\rm cl} + I_{\rm hom})/I_{\rm hom}$, where $I_{\rm cl}$ is the annihilation signal from the clumps, and $I_{\rm hom}$ that from homogeneously distributed DM particles with the NFW density profile in the Galactic halo. The main contribution to η is given by $\nu \simeq 2.5$ and $M \simeq M_{\rm min}$. The signal enhancement η is shown numerically in Figs. 3–5. One can see that for almost all allowed values of the primeval perturbation spectrum index $n_p \geqslant 1.0$ the annihilation signal from clumps gives the dominant contribution. This result does not depend on the properties of the DM particles.

The observations favor the spectrum index $n_p = 1.0$ [51]. Enhancement of the annihilation signal for this value of n_p is described by the factor 2–5 for different β with uncertainties due to the values of $M_{\rm min}$ and other parameters.

The clumps which give the dominant contribution to the annihilation signal have approximately the following properties in the case $n_p = 1$: the mass $M \sim M_{\rm min}$ and $\nu \sim 2.5$, the radius $R \simeq 3.6 \times 10^{15}$ cm, and the radius of the core $R_c \simeq 1.8 \times 10^{14}$ cm, the mean internal density of the clump $\overline{\rho}_{\rm int} \simeq 2.5 \times 10^{-22}$ g cm^{-3}, the fraction of the halo mass in the form of these clumps $\xi_{\rm int} \sim 0.002$, and the mean number density of these clumps in the halo $n_{\rm cl} \sim 25$ pc^{-3}.

Recently, the HEAT Collaboration detected an excessive flux of cosmic ray positrons at energy $E \sim 10$ GeV [56]. According to [57], if this positron flux is produced by annihilation of neutralinos an enhancement factor of the order of 30 is needed. The calculations presented here show that this enhancement can be reached in the scenario considered in the case of an extreme combination of parameters.

ACKNOWLEDGMENTS

This work has been supported in part by the INTAS Grant No. 99-1065; V.D. and Yu.E are supported also by the RFBR Grants No. 03-02-16436-a and 02-02-16762-a.

APPENDIX A: CROSS SECTIONS OF NEUTRALINO SCATTERING OFF ELECTRONS AND NEUTRINOS

As the neutralino we shall consider here a pure B-ino ($\chi = \tilde{B}$). The Lagrangian for interaction of the B-ino with left and right components of a fermion f can be written (see, e.g., [58,59]) as

$$\mathcal{L}_{f\tilde{f}\chi} = -g\sqrt{2} \tan\theta_W (e_f - T_{3f}^L) \overline{f} P_R \chi \tilde{f}_L + g\sqrt{2} \tan\theta_W e_f \overline{f} P_L \chi \tilde{f}_R , \tag{A1}$$

where g is the SU(2) coupling constant, θ_W is the Weinberg angle ($\sin^2\theta_W = 0.231$), e_f is the electric charge of the fermion f in units of the electron charge, T_{3f}^L is the projection of weak isospin for f_L, and $P_R = 1/2(1+\gamma_5)$ is a projection operator which cuts the left component from the operator $\overline{f}$ in Eq. (A1); $\tilde{f}_L$ is the left sfermion. The first term in the Lagrangian (A1) is $\mathcal{L}_{f_L \tilde{f}_L \chi}$, the second $\mathcal{L}_{f_R \bar{f}_R \chi}$. When f is ultrarelativistic in the frame where the neutralino is at rest, there is no interference for scattering of the left and right components of the fermions (the interference terms are proportional to m_f). Therefore, we shall calculate the $f\chi$ cross section for left f_L and right f_R fermions separately.

Scattering of the left fermion with $e_f = -1$ and $T_{3f} = -1/2$ (e.g., e, μ, τ) off the B-ino are described by the two

diagrams in the *s*- and *u* channels shown below:

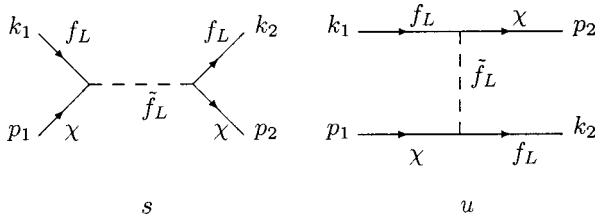

The standard calculations for matrix elements give for $|M|^2=|M_s|^2+|M_u|^2+2\,\mathrm{Re}(M_sM_u^*)$

$$|M_s|^2=\frac{1}{2}(g\tan\theta_W)^4\frac{(k_1p_1)(k_2p_2)}{(s-\tilde{m}_L^2)^2}, \tag{A2}$$

$$|M_u|^2=\frac{1}{2}(g\tan\theta_W)^4\frac{(p_1k_2)(k_1p_2)}{(s-\tilde{m}_L^2)^2}, \tag{A3}$$

$$M_sM_u^*=-\frac{1}{4}(g\tan\theta_W)^4\frac{m_\chi^2(k_1k_2)}{(s-\tilde{m}_L^2)(u-\tilde{m}_L^2)}. \tag{A4}$$

The cross section for the $f_L+\chi\to f_L+\chi$ scattering at angle θ_{12} in the system where the neutralino is at rest is given by

$$\left(\frac{d\sigma_{\rm el}}{d\Omega}\right)_{f_L\chi}=\frac{1}{64\pi^2 s}|M|^2=\frac{\alpha_{\rm e.m.}^2}{8\cos^4\theta_W}\frac{\omega^2(1+\cos\theta_{12})}{(m_\chi^2-\tilde{m}_L^2)^2}, \tag{A5}$$

where $\omega\gg m_f$ is the energy of f_L in the system where the neutralino is at rest, m_χ is the neutralino mass, and $\tilde{m}_L$ is the mass of the left sfermion.

Let us consider now $f_R+\chi\to f_R+\chi$ scattering described by the second term in the RHS of Eq. (A1). The diagrams are identical to that in the figure after substituting $f_L\to f_R$ and $\tilde{f}_L\to\tilde{f}_R$. Since traces do not change when $P_L\to P_R$, the expressions (A2)–(A4) remain the same, changing only due to the coupling constant which increases twice [see Eq. (A1)]. Therefore, we obtain

$$\left(\frac{d\sigma_{\rm el}}{d\Omega}\right)_{f_R\chi}=16\left(\frac{d\sigma_{\rm el}}{d\Omega}\right)_{f_L\chi}. \tag{A6}$$

In this paper we are interested in $\nu+\chi\to\nu+\chi$ and $e+\chi\to e+\chi$ scattering. In the former case the cross section is given by Eq. (A5), and in the latter case by the sum of $f_L+\chi\to f_L+\chi$ and $f_R+\chi\to f_R+\chi$ scattering, i.e., it is larger by a factor 17 than the cross section (A5).

APPENDIX B: KINETIC EQUATION

In this appendix we shall study the stage of kinetic equilibrium and the stage after its breaking in the common formalism of kinetic equations, similar to [42] and using the approach of [44]. We shall confirm in this way the results of Sec. III and clarify the difference in calculations of $M_{\rm min}$.

Following [44] we introduce the neutralino distribution function $f(x,p,t)$ over comoving coordinates $\vec{x}$ and momenta $\vec{p}=ma^2\dot{\vec{x}}$ (with this definition the momentum is constant for freely moving particles). The neutralino density is

$$\rho(x,t)=\frac{m}{a^3}\int d^3p\, f(x,p,t)=\overline{\rho_\chi}(t)[1+\delta(x,t)]. \tag{B1}$$

The kinetic equation with a collision term of the Fokker-Planck type [46] can be written as

$$\frac{\partial f}{\partial t}+\frac{p_i}{ma^2}\frac{\partial f}{\partial x_i}-m\frac{\partial\phi}{\partial x_i}\frac{\partial f}{\partial p_i}=D_p(t)\frac{\partial}{\partial p_i}\left(\frac{p_i}{mTa^2}f+\frac{\partial f}{\partial p_i}\right), \tag{B2}$$

where ϕ is the gravitational potential, which can be neglected at the considered epoch $t\leqslant t_{\rm eq}$, $T(t)$ is the temperature of the ambient plasma given by Eq. (18), and $D_p(t)$ is the diffusion coefficient in momentum space. According to [46]

$$D_p(t)=\frac{40}{3}\int d\Omega\int d\omega\, n_0(\omega)\left(\frac{d\sigma_{\rm el}}{d\Omega}\right)_{f_L\chi}(\delta p)^2. \tag{B3}$$

The number 40 in Eq. (B3) comes from the counting of degrees of freedom in neutralino-fermion scattering as in Sec. III.

Equation (B2) with the diffusion coefficient (B3) coincides with Eq. (16) from [42] except for the numerical factor in D_p which is of the order of unity.

1. Kinetic decoupling

Let us consider the exit of neutralinos from kinetic equilibrium (decoupling) in the homogeneous universe, when the $\partial/\partial x_i$ terms in Eq. (B2) can be neglected. The temperature of the neutralino gas T_χ is defined as

$$\int p_ip_jf\,d^3p=\tilde{\rho}_\chi a^5T_\chi(t)S_{ij}. \tag{B4}$$

Multiplying Eq. (B2) by p_ip_j and integrating it over d^3p one obtains

$$\frac{dT_\chi}{dt}+2\frac{\dot{a}}{a}T_\chi-\frac{2D_p(t)}{ma^2}\left(1-\frac{T_\chi(t)}{T(t)}\right)=0, \tag{B5}$$

The initial condition for Eq. (B5) can be chosen at the moment of freezing $t=t_f$ as in [42], or more conveniently at any t_i from the interval $t_f<t_i\ll t_d$, as $T_\chi(t_i)=T(t_i)$, where T is the temperature of ambient plasma. Solution of Eq. (B5) (see below) causes transition of the ratio $r(t)=T_\chi(t)/T(t)$ from $r=1$ to $r_d<1$ within some time interval, determined by r_d. Any value of t in this interval can be taken as the definition of decoupling time t_d. Equation (B5) and its solution can be simplified using the dimensionless time $\tau=t/t_d$. The characteristic time t_d naturally emerges from the dimensional parameters entering the diffusion coefficient, and up to a numerical coefficient it coincides with t_d determined in Sec. III. The transition time interval fixes this numerical coefficient with some uncertainty, and we indeed obtain t_d [and hence

$T_d = T(t_d)$] approximately equal to those given by Eqs. (19) and (20) in Sec. III. The solution of Eq. (B5) in terms of $\tau = t/t_d$ is given by

$$\frac{T_\chi(t)}{T_d} = \frac{1}{\tau}\left(\tau_i^{-1/2} e^{1/4\tau^2 - 1/4\tau_i^2} + \frac{1}{2} e^{1/4\tau^2} \int_{\tau_i}^{\tau} d^3x\, x^{-5/2} e^{1/4x^2} \right). \tag{B6}$$

The asymptotic forms of the solution (B6) are given by $T_\chi/T_d = \tau^{-1/2}$ for $\tau \ll 1$ and $T_\chi/T_d = \tau^{-1}\Gamma(3/4)/2^{1/2}$ for $\tau \gg 1$, as they must be. From the solution (B6) it is seen that the transition from kinetic equilibrium of the neutralino with relativistic fermions to the nonequilibrium regime proceeds very fast. For this reason our consideration of diffusion and free streaming independently in Sec. III is well justified.

2. Diffusion

Consider Eq. (B2) before kinetic decoupling, $t \ll t_d$. One can find the first two moments by integrating Eq. (B2) first over d^3p and second over $p_i d^3p$. Inserting the first of the equations obtained into the second one we obtain the following equation for the Fourier components:

$$\frac{\partial^2 \delta}{\partial^2 t} + 2\frac{\dot{a}}{a}\frac{\partial \delta}{\partial t} + D_p(t)\frac{1}{mTa^2}\frac{\partial \delta}{\partial t} = \frac{k_i k_j}{\overline{\rho_\chi} a^7 m} \int p_i p_j f\, d^3p. \tag{B7}$$

The RHS of Eq. (B7) has the tensor form

$$\frac{1}{\overline{\rho_\chi} a^7 m} \int p_i p_j f\, d^3p = E\,\delta_{ij} + F k_i k_j, \tag{B8}$$

where the isotropic part $E = T_\chi \delta_k / a^2 m$ for any τ, while F depends on time t. In the limit $\tau \ll 1$ we may put $F = 0$ and neglect the first and second terms in Eq. (B7). The resultant equation coincides with the diffusion equation (24) with the same diffusion coefficient (23) and has the same solution.

In [42] only this diffusion limit of the general kinetic equation (B2) has been considered.

3. Free streaming

In the limiting case $\tau \gg 1$, i.e., after decoupling, Eq. (B2) has the simple form

$$\frac{\partial f}{\partial t} + \frac{p_i}{ma^2}\frac{\partial f}{\partial x_i} = 0, \tag{B9}$$

with the solution

$$f \propto \exp\left[\frac{i k_j p_j}{m a_d} g(t) \right], \tag{B10}$$

where $g(t)$ is the same function as Eq. (28). The solution (B10) is valid with a good accuracy at $\tau \geqslant 1$ also, because according to Eq. (B6), kinetic decoupling proceeds very fast. Integrating Eq. (B10) over d^3p with the initial condition

$$f(t_d) = (2\pi T_d m a_d^2)^{-3/2} \exp\left\{ -\frac{p^2}{2 T_d m a_d^2} \right\}, \tag{B11}$$

one obtains

$$n_{\vec{k}}(t) = n_{\vec{k}}(t_d) e^{-(1/2)k^2 g^2(t) T_d / m_\chi}, \tag{B12}$$

and then Eqs. (33), (34), and (38) from Sec. III.

[1] J. Silk and A. Stebbins, Astrophys. J. **411**, 439 (1993).
[2] A. V. Gurevich, K. P. Zybin, and V. A. Sirota, Sov. Phys. Usp. **167**, 913 (1997).
[3] B. Moore *et al.*, Astrophys. J. Lett. **524**, L19 (1999).
[4] S. Ghigna, B. Moore, F. Governato, G. Lake, T. Quinn, and J. Stadel, Astrophys. J. **544**, 616 (2000).
[5] A. Klypin, S. Gottlober, A. V. Kravtsov, and A. M. Khokhlov, Astrophys. J. **516**, 530 (2002).
[6] E. Bertschinger, Astrophys. J., Suppl. Ser. **58**, 39 (1985).
[7] Y. Hoffman and J. Shaham, Astrophys. J. **297**, 16 (1985).
[8] B. S. Ryden and J. E. Gunn, Astrophys. J. **318**, 15 (1987).
[9] A. V. Gurevich and K. P. Zybin, Sov. Phys. Usp. **165**, 723 (1995).
[10] J. F. Navarro, C. S. Frenk, and S. D. M. White, Astrophys. J. **462**, 563 (1996).
[11] D. D. Kelson *et al.*, Astrophys. J. **576**, 720 (2002).
[12] Y. P. Jing and Y. Suto, Astrophys. J. Lett. **529**, L69 (2000).
[13] D. Syer and S. D. M. White, Mon. Not. R. Astron. Soc. **293**, 337 (1998).
[14] A. Dekel, I. Arad, J. Devor, and Y. Birnboim, astro-ph/0205448.
[15] J. E. Taylor and J. F. Navarro, Astrophys. J. **563**, 483 (2001).
[16] V. S. Berezinsky, A. V. Gurevich, and K. P. Zybin, Phys. Lett. B **294**, 221 (1992).
[17] V. Berezinsky, A. Bottino, and G. Mignola, Phys. Lett. B **325**, 136 (1994).
[18] L. Bergstrom, J. Edsjo, P. Gondolo, and P. Ulio, Phys. Rev. D **59**, 043506 (1999).
[19] P. Gondolo and J. Silk, Phys. Rev. Lett. **83**, 1719 (1999).
[20] P. Ullio, H. Zhao, and M. Kamionkowski, Phys. Rev. D **64**, 043504 (2001).
[21] G. Bertone, G. Sigl, and J. Silk, Mon. Not. R. Astron. Soc. **337**, 98 (2002).
[22] D. Merritt, M. Milosavljevic, L. Verde, and R. Jimenez, Phys. Rev. Lett. **88**, 191301 (2002).
[23] V. Berezinsky, A. Bottino, and G. Mignola, Phys. Lett. B **391**, 355 (1997).
[24] G. Jungman and M. Kaminkowski, Phys. Rev. D **49**, 2316 (1994).
[25] A. Bottino, C. Favero, N. Fornengo, and G. Mignola, Astropart. Phys. **3**, 77 (1995).
[26] A. Bottino, F. Donato, N. Fornengo, and P. Salati, Phys. Rev. D **58**, 123503 (1998).
[27] R. Aloisio, P. Blasi, and A. V. Olinto, astro-ph/0206036.
[28] A. Tasitsiomi and A. V. Olinto, Phys. Rev. D **66**, 083006 (2002).
[29] J. E. Taylor and J. Silk, Mon. Not. R. Astron. Soc. **339**, 505 (2003).

[30] L. Bergstrom, J. Edsjo, and P. Ulio, Phys. Rev. D **58**, 083507 (1998).
[31] L. Bergstrom, J. Edsjo, and C. Gunnarsson, Phys. Rev. D **63**, 083515 (2001).
[32] P. Ullio, L. Bergstrom, J. Edsjo, and C. Lacey, Phys. Rev. D **66**, 123502 (2002).
[33] P. Blasi, A. V. Olinto, and C. Tyler, Astropart. Phys. **15**, 649 (2003).
[34] B. L. Carr and C. C. Lacey, Astrophys. J. **316**, 23 (1987).
[35] E. Ardi, T. Tsuchiya, and A. Burkert, astro-ph/0206026.
[36] E. W. Kolb and I. I. Tkachev, Phys. Rev. D **50**, 769 (1994).
[37] V. I. Dokuchaev and Yu. N. Eroshenko, JETP **94**, 1 (2002).
[38] W. H. Press and P. Schechter, Astrophys. J. **187**, 425 (1974).
[39] J. R. Bond, S. Cole, G. Efstathiou, and N. Kaiser, Astrophys. J. **379**, 440 (1991).
[40] C. Lacey and S. Cole, Mon. Not. R. Astron. Soc. **262**, 627 (1993).
[41] J. E. Gunn *et al.*, Astrophys. J. **223**, 1015 (1978).
[42] K. P. Zybin, M. I. Vysotsky, and A. V. Gurevich, Phys. Lett. A **260**, 262 (1999).
[43] S. Hofmann, D. J. Schwarz, and H. Stocker, Phys. Rev. D **64**, 083507 (2001).
[44] P. J. E. Peebles, *Large-Scale Structure of the Universe* (Princeton University Press, Princeton, NJ, 1993)
[45] B. Moore *et al.*, Astrophys. J. Lett. **524**, L19 (1999).
[46] L. D. Landau, E. M. Lifshits, and L. P. Pitaevsky, *Physical Kinetics*, Course of Theoretical Physics Vol. 10 (Pergamon Press, Oxford, 1981).
[47] J. M. Bardeen *et al.*, Astrophys. J. **304**, 15 (1986).
[48] A. Burkert, Astrophys. J. Lett. **447**, L25 (1995).
[49] W. J. G. de Blok, A. Bosma, and S. S. McGaugh astro-ph/0212102.
[50] O. Y. Gnedin, L. Hernquist, and J. P. Ostriker, Astrophys. J. **514**, 109 (1999).
[51] D. N. Spergel *et al.*, Astrophys. J., Suppl. Ser. **148**, 175 (2003).
[52] E. V. Bugaev and K. V. Konishchev, Phys. Rev. D **65**, 123005 (2002).
[53] C. Schmid, D. J. Schwarz, and P. Widerin, Phys. Rev. D **59**, 043517 (1999).
[54] V. S. Berezinsky and A. A. Mikhailov, Phys. Lett. B **449**, 237 (1999).
[55] C. G. Lacey and J. P. Ostriker, Astrophys. J. **299**, 633 (1985).
[56] HEAT-pbar Collaboration, S. Coutu *et al.*, in Proceedings of 27th ICRC, 2001.
[57] E. A. Baltz, J. Edsjoet, K. Freese, and P. Gondolo, astro-ph/0211239.
[58] G. Jungman, M. Kamionkowski, and K. Griest, Phys. Rep. **267**, 195 (1996).
[59] H. E. Haber and G. L. Kane, Phys. Rep. **117**, 75 (1985).